NASA/TM-2006-214524

Determination of Extrapolation Distance With Pressure Signatures Measured at Two to Twenty Span Lengths From Two Low-Boom Models

Robert J. Mack and Neil S. Kuhn
Langley Research Center, Hampton, Virginia

November 2006

The NASA STI Program Office . . . in Profile

Since its founding, NASA has been dedicated to the advancement of aeronautics and space science. The NASA Scientific and Technical Information (STI) Program Office plays a key part in helping NASA maintain this important role.

The NASA STI Program Office is operated by Langley Research Center, the lead center for NASA's scientific and technical information. The NASA STI Program Office provides access to the NASA STI Database, the largest collection of aeronautical and space science STI in the world. The Program Office is also NASA's institutional mechanism for disseminating the results of its research and development activities. These results are published by NASA in the NASA STI Report Series, which includes the following report types:

- TECHNICAL PUBLICATION. Reports of completed research or a major significant phase of research that present the results of NASA programs and include extensive data or theoretical analysis. Includes compilations of significant scientific and technical data and information deemed to be of continuing reference value. NASA counterpart of peer-reviewed formal professional papers, but having less stringent limitations on manuscript length and extent of graphic presentations.

- TECHNICAL MEMORANDUM. Scientific and technical findings that are preliminary or of specialized interest, e.g., quick release reports, working papers, and bibliographies that contain minimal annotation. Does not contain extensive analysis.

- CONTRACTOR REPORT. Scientific and technical findings by NASA-sponsored contractors and grantees.

- CONFERENCE PUBLICATION. Collected papers from scientific and technical conferences, symposia, seminars, or other meetings sponsored or co-sponsored by NASA.

- SPECIAL PUBLICATION. Scientific, technical, or historical information from NASA programs, projects, and missions, often concerned with subjects having substantial public interest.

- TECHNICAL TRANSLATION. English-language translations of foreign scientific and technical material pertinent to NASA's mission.

Specialized services that complement the STI Program Office's diverse offerings include creating custom thesauri, building customized databases, organizing and publishing research results ... even providing videos.

For more information about the NASA STI Program Office, see the following:

- Access the NASA STI Program Home Page at ***http://www.sti.nasa.gov***

- E-mail your question via the Internet to help@sti.nasa.gov

- Fax your question to the NASA STI Help Desk at (301) 621-0134

- Phone the NASA STI Help Desk at (301) 621-0390

- Write to:
  NASA STI Help Desk
  NASA Center for AeroSpace Information
  7121 Standard Drive
  Hanover, MD 21076-1320

NASA/TM-2006-214524

Determination of Extrapolation Distance With Pressure Signatures Measured at Two to Twenty Span Lengths From Two Low-Boom Models

Robert J. Mack and Neil S. Kuhn
Langley Research Center, Hampton, Virginia

National Aeronautics and
Space Administration

Langley Research Center
Hampton, Virginia 23681-2199

November 2006

Available from:

NASA Center for AeroSpace Information (CASI)
7121 Standard Drive
Hanover, MD 21076-1320
(301) 621-0390

National Technical Information Service (NTIS)
5285 Port Royal Road
Springfield, VA 22161-2171
(703) 605-6000

Summary

A study was performed to determine a limiting separation distance between wind-tunnel model and survey probe for the practical extrapolation of pressure signatures from cruise altitude to the ground. The study was performed at two wind-tunnel facilities with two low-boom-tailored models designed to generate ground pressure signatures with "flattop" shapes. Data from the first wind-tunnel facility came from separation distances of 2 to 5 span lengths. They showed measured pressure signatures that had not achieved the desired low-boom features that could be accurately extrapolated. However, the second wind-tunnel facility provided pressure signatures with shapes that indicated a limiting extrapolation distance was within the test separation distance range of 5 to 20 span lengths. Pressure signatures measured at separation distances equal to, or greater than, this limiting distance could readily be extrapolated to obtain credible predictions of ground overpressures.

Introduction

Several methods are presently used for extrapolating near-field pressure signatures from cruise altitude to the ground. The first method, and the one most often used, is the Thomas Code, reference 1. A second is the Ames Code, reference 2. These two methods use inputs of a near-field pressure signature, the cruise altitude, and the cruise Mach number. They produce credible ground overpressure predictions for slender bodies of revolution.

A third method is the Aeronautical Research Associates of Princeton (ARAP) Code, reference 3. This method employs inputs of a body's Whitham F-function, reference 4, or the body's equivalent areas along with the cruise altitude and the Mach number to predict ground pressure signatures. It is seldom used to extrapolate a near-field pressure signature or an F-function derived from a wind-tunnel-measured pressure signature.

However, the situation is very different when the near-field pressure signature is generated by an aircraft in supersonic cruise flight, by a lifting wing-body model in a supersonic wind tunnel, or by a Computational Fluid Dynamics (CFD) code using a numerical representation of a concept's or a wind-tunnel model's geometry. In these cases, the flow field close to the body is highly three-dimensional in nature. So, the first two of these three extrapolation methods cannot be properly applied because they are based on the same cylindrical acoustic propagation model in the theory developed by G. B. Whitham, reference 4, and extended by F. Walkden, reference 5. However, if pressure signatures were measured, or predicted, at a sufficiently-large distance where the local flow has become quasi-two-dimensional in nature and the pressure signature's low-boom shape features have largely been established, the extrapolation process could provide credible results. This "limiting distance" could also be defined as the distance where the shape of the signatures, measured directly under the flight path of the model, would have developed (or settled into) the cruise-field's quasi-two-dimensional form. At or beyond this limiting distance, the measured pressure signatures or numerically calculated pressure signatures extrapolated with these methods could provide credible ground overpressure predictions.

Such a limiting distance could be determined by a couple of methods. The first method would employ numerical CFD studies where attenuation trends could be monitored. A second method would be to measure wind-tunnel-model pressure signatures over a range of increasing separation distances. A limiting distance determined by either method could be expressed as distance/span ratio since the three-dimensional nature of the configuration's flow field is determined mainly by the lift developed across the span, even though the longitudinal distribution of the lift is also an important effect. By low-boom tailoring the model's wing-fuselage geometry for a "flattop" ground signature, the shape characteristics of the pressure signature would be reasonably easy to monitor as the separation distance was increased in the wind-tunnel test section.

A study to determine such a limiting distance by the second of these previously mentioned methods was begun in 2001. It was to be performed at two facilities, the Langley Research Center Unitary Plan Wind Tunnel Facility, and the John Glenn Research Center 10 ft x 10 ft Wind Tunnel Facility. The first half of the study was performed and reported in reference 6. In this report, the data obtained in both the Langley Research Center Facility and in the John Glenn Research Center Facility were presented, analyzed, and discussed. Results from this analysis were the basis for conclusions, predictions, and recommendations.

Nomenclature

b	wing span of the models, 4.5 in
C_L	lift coefficient
$C_{L,CRUISE}$	lift coefficient at cruise
$F(y)$	value of the Whitham F-function at effective distance y, $ft^{1/2}$
h	vertical separation distance between the model nose and flight-track probe, in
I	non dimensional pressure signature impulse, $I = \int_0^{\tau_o} \frac{\Delta p}{p} d\tau$
l	overall length of the models, nose to wing-tip trailing edge, 9.0 in
l_e	effective length of the models at $C_{L,CRUISE}$, 9.0 in
M	cruise Mach number
p	ambient pressure, psf
p_{REF}	static pressure measured by the wall-mounted reference probe, psf
p_{TS}	static pressure in the center of the test-section, psf
Δp	incremental free-stream overpressure, psf
S	wing projected area, in^2
x	distance in the longitudinal direction, in
x_o	longitudinal distance where the impulse is a maximum, in
y	distance in the spanwise direction normal to x , in, or effective distance, ft
τ	dimensionless dummy variable, x / l_e , in the equation of the impulse
τ_o	dimensionless ratio, x_o / l_e , along the pressure signature where the impulse, I , is a maximum

Abbreviations

CLE	Curved Leading Edge
SLSLE	Straight Line Segmented Leading Edge
JGRC	John Glenn Research Center
LaRC	Langley Research Center

Concept And Model Design

Concept Design

Two concepts were designed for this study to determine a limiting distance for extrapolation of wind-tunnel-measured pressure signatures. Both concepts had the same wing area, wing span, lifting length, and thickness-to-chord ratio. Nacelles and fins were omitted, so only wing-fuselage volume and wing lift effects were present. These simplified wing-fuselage configurations were then low-boom tailored to produce a ground overpressure of 0.5 psf. This was the same ground overpressure level that a recently-designed Supersonic Business Jet (SBJ) Concept, reference 7, produced at a cruise Mach number of 2.0, a beginning-cruise weight of 88,500 lb, and a beginning-cruise altitude of 53,000 feet.

The two concepts had one major difference. One concept had a wing with a smooth and continuous leading edge, the Curved Leading Edge (CLE) model, while the other concept had a wing with a straight-line segmented leading edge, the Straight-Line Segmented Leading Edge (SLSLE) model. These wings are shown in figure 1.

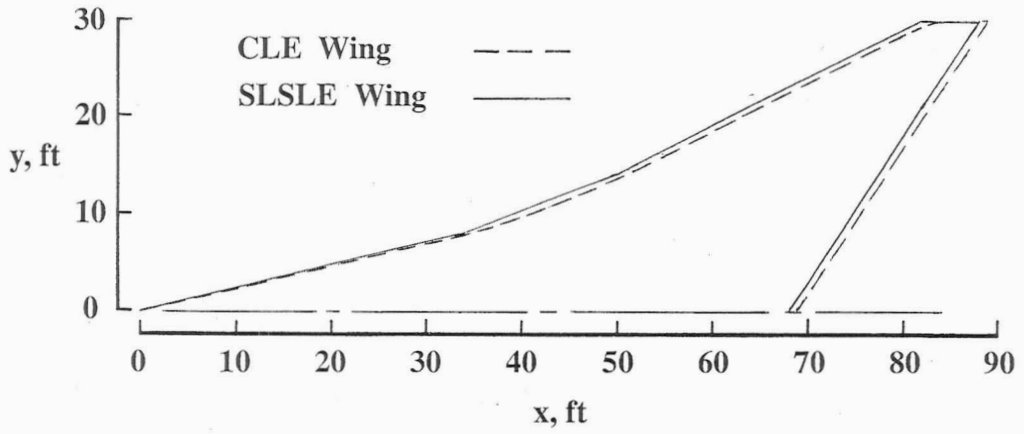

Figure 1. Wing planforms of the two concepts and wind-tunnel models, full-scale dimensions.

Extra equivalent area was added to the concepts' total equivalent area due to wing-fuselage volume and wing lift to account for the sting that would support the models in the wind-tunnel test section. Using the code described in reference 8, and developed in references 9 and 10, the fuselage volume received most of the low-boom tailoring. When completed, the volume equivalent areas from the wing, fuselage, and forward sting section, along with the equivalent area from the wing lift, closely matched the concepts' equivalent area profile required for the desired low-boom overpressures and pressure signature shape. Dihedral, shown to be useful for achieving low-boom performance, references 11 and 12, was added to the wing-body models to make the wing tip trailing edges and the model nose lay in a plane parallel with the free-stream velocity vector. This design feature assured the concepts' and the models' overall lengths and the effective lengths would be equal, i.e. $l = l_e$, at Mach 2 and $C_L = C_{L,CRUISE}$.

A comparison of the ideal and the designed equivalent areas for both concepts are presented in figure 2.

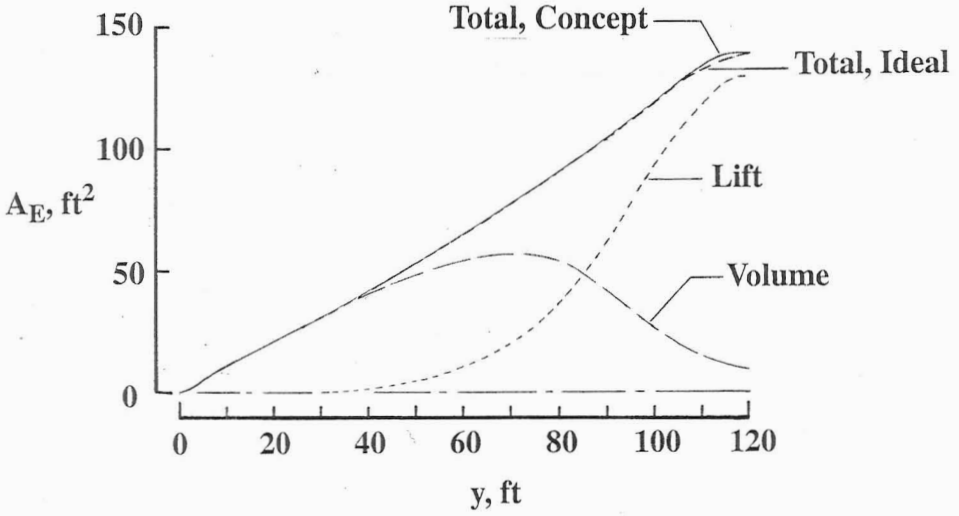

(a) Curved Leading Edge (CLE) concept.

Figure 2. Comparison of ideal and concept equivalent areas.

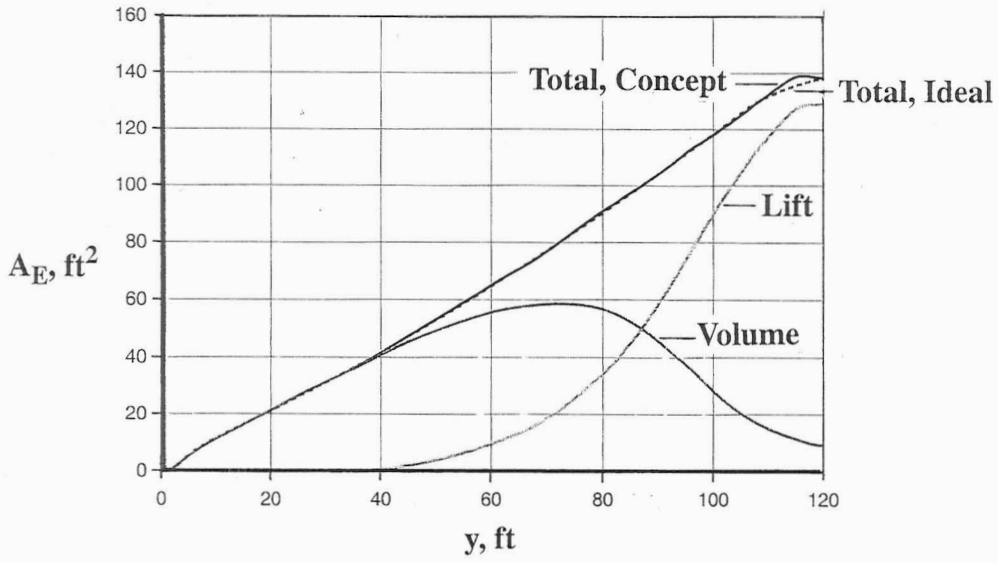

(b) Straight-Line Segmented Leading Edge (SLSLE) concept.

Figure 2. Concluded.

In figures 2(a) and 2(b), the ideal and design equivalent area curves matched very closely along the equivalent length of the concepts. Each concept had finite wing/body thicknesses and wing lift "Mach sliced" by planes inclined at a Mach angle of 30 degrees to the horizontal reference plane to develope the equivalent areas. Fuselage contours were adjusted by "hand tailoring" of normal areas to obtain a close match between ideal and designed equivalent areas. When Whitham F-functions were calculated from these equivalent areas, each small difference produced a local "irregularity" in the desired equivalent area curve. This is seen in figure 3.

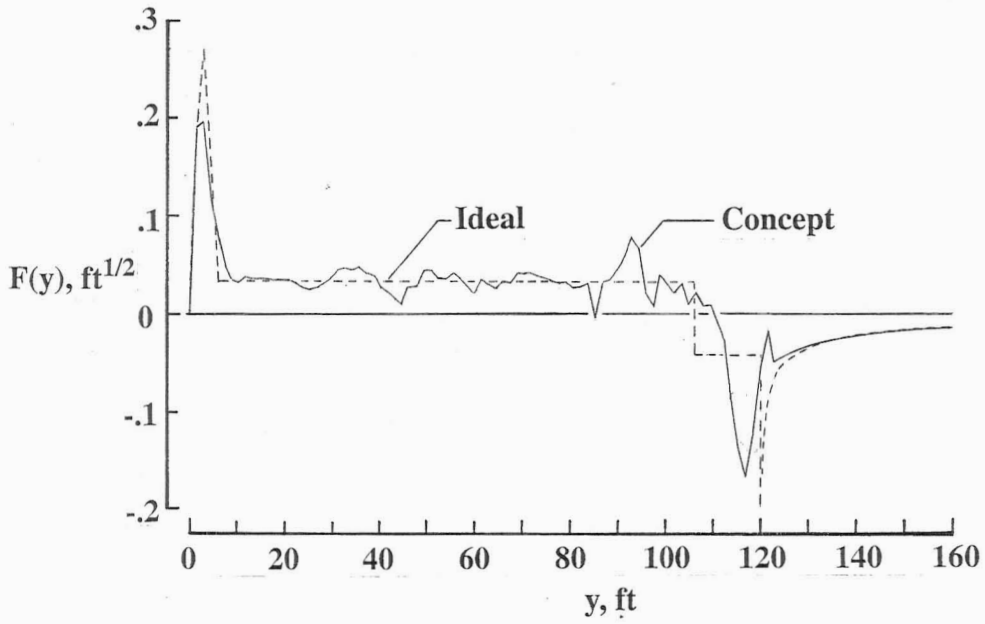

(a) Curved Leading Edge (CLE) concept.

Figure 3. Comparison of ideal and concept F-functions.

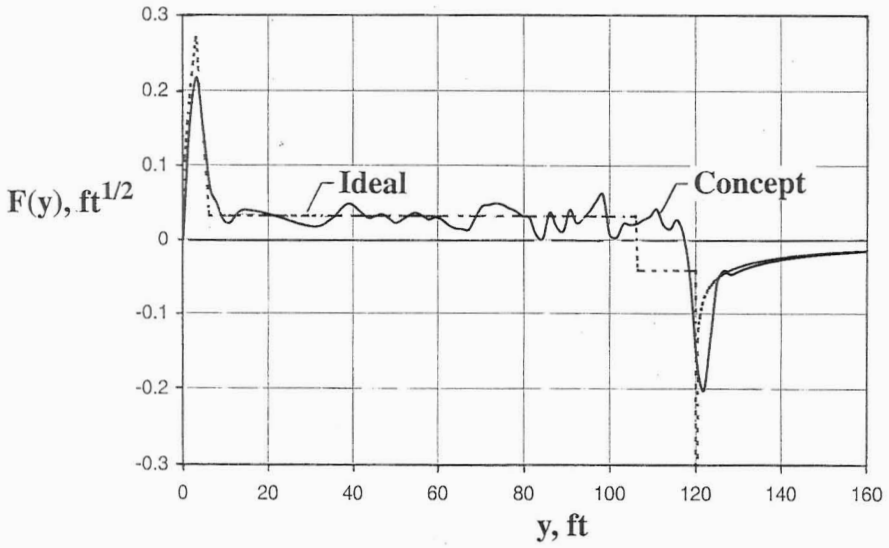

(b) Straight-Line Segmented Leading Edge (SLSLE) concept.

Figure 3. Concluded.

When the ground pressure signatures were calculated from the individual Whitham F-functions, these "irregularities" appeared on the shapes of the pressure signatures. This propagational "carry-over" is seen in figure 4.

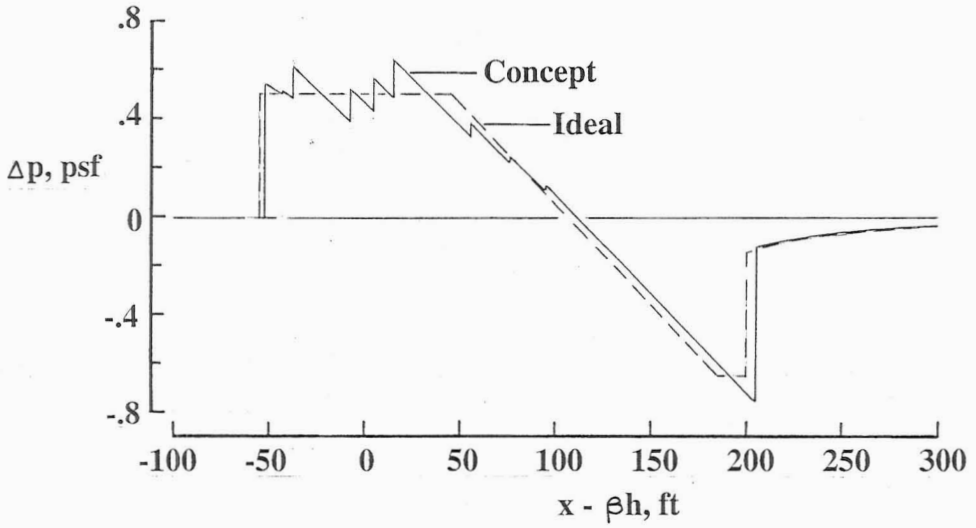

(a) Curved Leading Edge (CLE) concept.

Figure 4. Comparison of ideal and designed ground overpressure signatures.

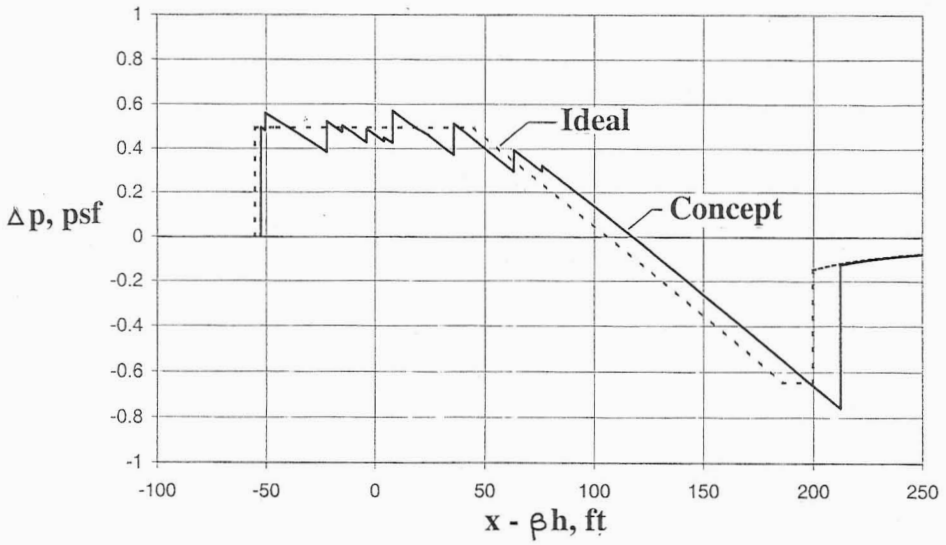

(b) Straight-Line Segmented Leading Edge (SLSLE) concept.

Figure 4. Concluded.

Although computational in nature, these "irregularities" were retained as reference features.

Wind-Tunnel Model Design

After the wing-fuselage concepts had been designed, their dimensions were rescaled by a factor of 1:160 so wind-tunnel models could be built. Both wind-tunnel models were supported by a sting/balance whose surface contours merged with the areas and slopes on the rescaled concepts' aft fuselages. Each model and sting/balance was 32 inches in length with a 4-inch long, 0.75-inch diameter mounting stub at the back of the sting/balance. The wing and fuselage of the CLE model attached to a cylindrical section is shown in figure 5.

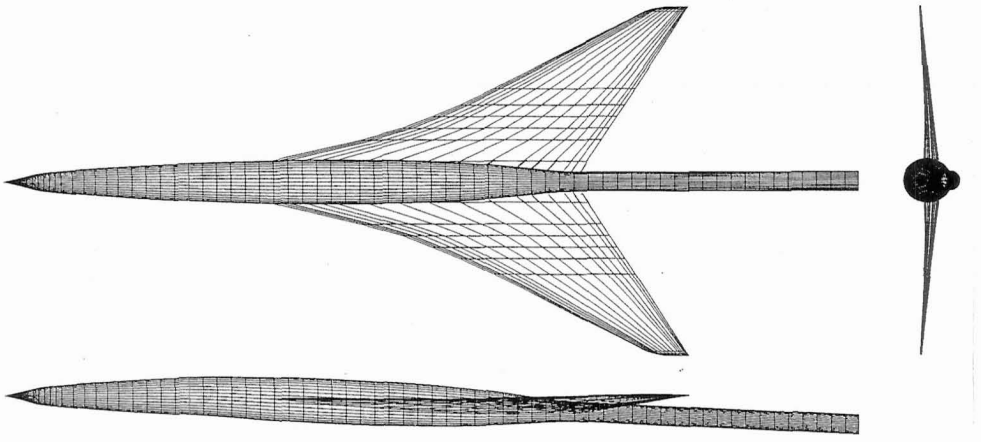

Figure 5. Three-view schematic of the CLE model.

The SLSLE model was similar in shape to the CLE model. This similarity is seen by comparing the three-view of the CLE model, figure 5, with the three-view of the SLSLE model in figure 6.

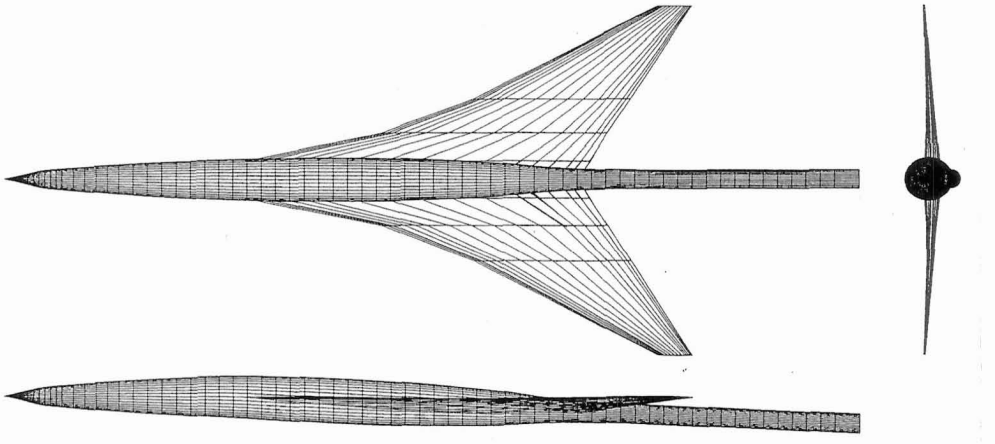

Figure 6. Three-view schematic of the SLSLE model.

Full-scale concept flight data and wind-tunnel model dimensions are listed in Appendix A. Numerical descriptions of each model are given (in Wave Drag code format, references 13 and 14) in Appendix B and Appendix C.

Except for the leading edge shapes, the two concepts and models were virtually identical. However, the effects of different leading edge shapes was one of the issues addressed in this study. Seebass and George Minimization Theory curves have a smooth and continuous growth of volume and lift equivalent areas over most of the concept's effective length for control of the pressure signature's low-boom shape. Since the wing lift provided such an important contribution to the total equivalent areas, it would be desirable for the lift development gradients to be smooth and continuous. This strongly suggested that the wing have a smoothly-continuous, subsonic leading edge. However, it would be easier to build a wing whose leading edge had straight-line segments than a wing whose leading edge was smooth and continuous from wing-fuselage

junction to tip. If it could be shown that a straight-line segmented wing leading edge added few penalties to the aerodynamic performance and the low-boom ground overpressures, then the disadvantages of having a smooth and continuous wing leading edge could be avoided.

Wind Tunnel Facilities

Wind-Tunnel Test Sections

In the wind-tunnel test section, the models' stings were mounted on an angle-of-attack mechanism that controlled the lift by altering the model's flight attitude. This angle-of-attack mechanism was carried on its own sting attached to the wind-tunnel strut mechanism. In both the Langley Research Center Unitary Plan Wind Tunnel Facility and the John Glenn Research Center 10 ft x 10 ft Wind Tunnel Facility, the strut mechanism was set at the desired separation distance, and then translated longitudinally to permit the measurement of the overpressure points that defined a pressure signature.

Schematics of the wind-tunnel test section arrangements of model and measurement apparatus in the Langley Facility are shown in figures 7(a) and 7(b).

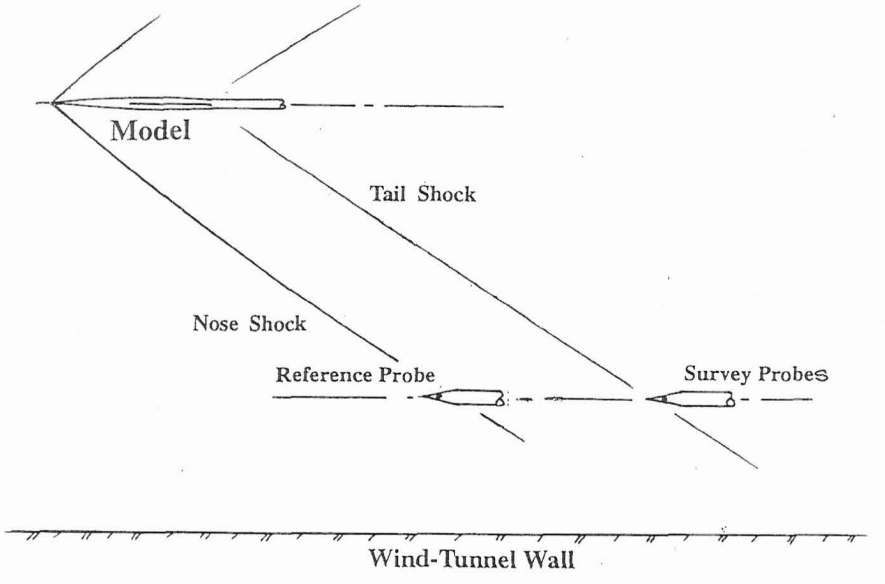

(a) Side view of model and probes in the Langley Facility test section.

Figure 7. Schematics of model and probes in the Langley Facility test section.

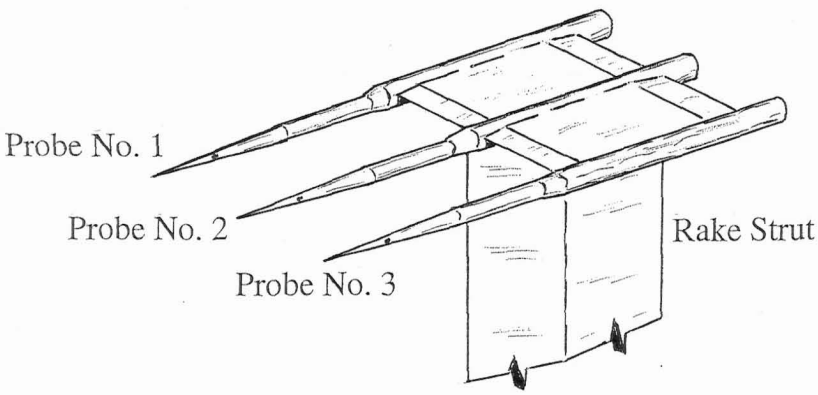

(b) Schematic of the survey probe rake and probes in the Langley Facility test section.

Figure 7. Concluded.

Three conical survey probes were used to measure pressure signatures. They were mounted side by side on a rake in a plane normal to the model's vertical plane of symmetry. This rake sat on a mast attached to the side wall. Survey Probe No. 1 measured pressure signatures along a line below and 2.95 inches to the right of the model; Survey Probe No. 2 measured pressure signatures along a line directly under the model; and Survey Probe No. 3 measured pressure signatures along a line below and 6.35 inches to the left of the model. Probe No. 1 was located between Probe No. 2, and the conical reference probe mounted on a mast to the test-section side wall.

The arrangement of wind-tunnel test section apparatus in the John Glenn Facility is shown in figures 8(a) and 8(b).

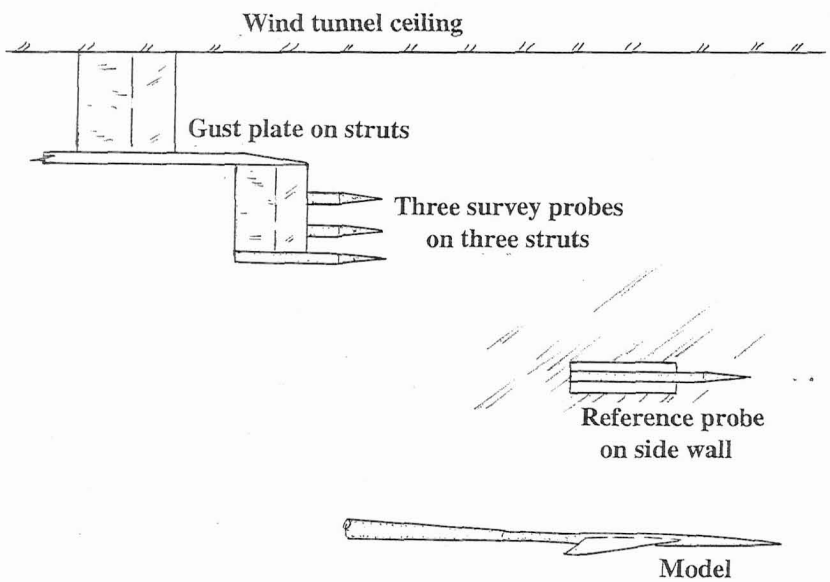

(a) Side-view sketch of model and probes in the John Glenn Facility test section.

Figure 8. Schematics of model and probes in the John Glenn Facility test section.

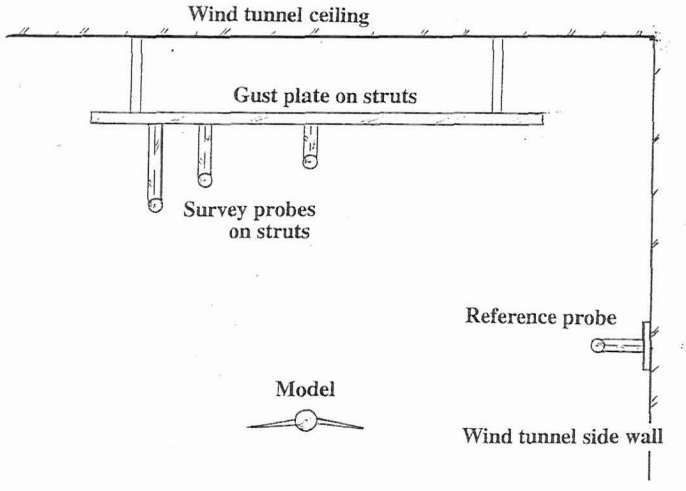

(b) Front view sketch of the model and probes in the John Glenn Facility test section.

Figure 8. Concluded.

Again, three two-orifice conical probes were used to measure the pressure signatures. They were mounted on masts attached to a horizontal "gust plate" hung from the ceiling of the test section. Survey Probe No. 1 measured pressure signatures under the model and was hung 2 inches below the gust plate; Survey Probe No. 2 measured signatures along a line 18 inches to the left of the model and was hung 4 inches below the gust plate; and Survey Probe No. 3 measured signatures along a line 27 inches to the left of the model and was hung 6 inches below the gust plate. The Reference Static Pressure Probe was mounted on the test section side wall opposite the wind-tunnel side wall near the outer two probes.

In this report, only the under-the-flight track pressure signatures measured at $C_{L,CRUISE}$ with Probe No. 2 in the Langley Facility, and with Probe No. 1 in the John Glenn Facility will be presented, discussed, and analyzed. However, all the measured pressure signatures are available for present and future CFD code validation. These measured pressure signature data were recorded electronically, and CD copies can be obtained by request.

Pressure Signature Measurements

Pressure Signature Matrix

Pressure signatures were measured at Mach 2 at four separation distances in the Langley Facility, and at four separation distances in the John Glenn Facility. Two C_L / $C_{L,CRUISE}$ ratios were also used to determine the influence and relative importance of lift on the shape of the pressure signature with increasing separation distance. These measured pressure signatures would be used to determine how, and at what rate, the pressure signature shapes "aged" (changed) as model/survey probe(s) separation distance(s) increased. Due to the large volume of data obtained, only the pressure signatures measured directly under the flight track and at C_L / $C_{L,CRUISE}$ = 1.0 are presented and analyzed in this report. Tables presented in Appendix D and Appendix E, list

the under-the-track separation distances and the two $C_L / C_{L,CRUISE}$ ratios used to measure the pressure signatures generated by each of the models.

Pressure Signatures

The sample of measured pressure signatures selected for analysis, comparison with theory, and discussion were those measured under the models' flight path at $C_L / C_{L,CRUISE} = 1.0$. Pressure signatures from the CLE model were measured at the Langley Facility, but not at the John Glenn Facility. A temperature-compensation failure in the strain gauges measuring normal force and pitching moment was discovered during measurements of pressure signatures at a separation distance of 22.5 inches. This defect was confirmed after the aborted test during an examination of the model's strain-gauge balance at room and at operating temperatures.

A pressure signature from the SLSLE model was measured in the John Glenn Facility wind tunnel at a separation distance of 22.5 inches and compared with the pressure signature measured in the Langley Facility wind tunnel at the same separation distance. These two measured pressure signatures are shown and compared in figure 9.

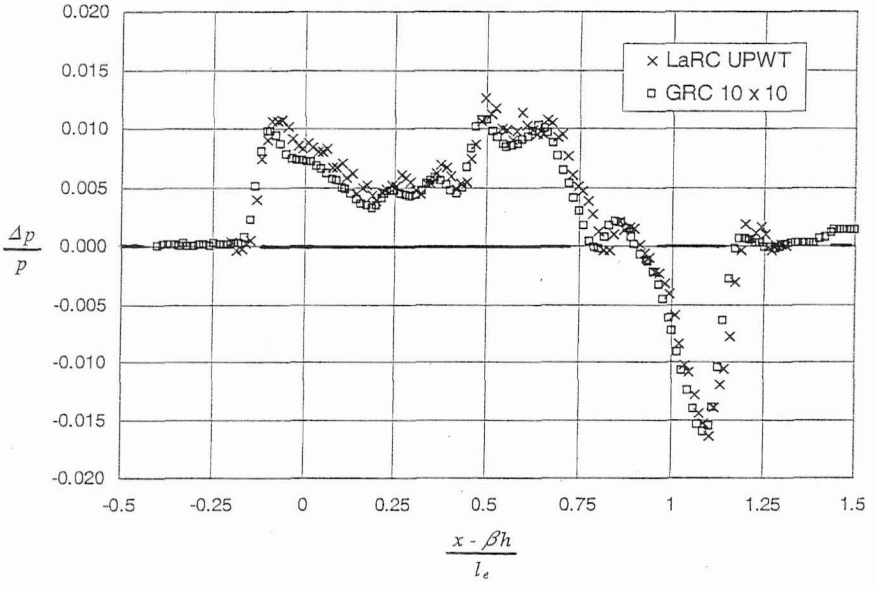

Figure 9. Comparison of pressure signatures from the SLSLE model. M = 2, h = 22.5 inches, and $C_L / C_{L,CRUISE} = 1.0$.

The shapes of the two pressure signature are almost the same, with reasonably good overall agreement in signature length, overpressure magnitudes, and shock locations.

The pressure signature measurement apparatus, shown in figure 8, was employed for the first time in the 10 ft x 10 ft Supersonic Wind Tunnel Facility at the John Glenn Research Center. To determine the flow quality in the test section at Mach 2 along the same path the research models would travel when their pressure signatures were measured, a cone-cylinder model, shown in figure 10, was designed, built and tested.

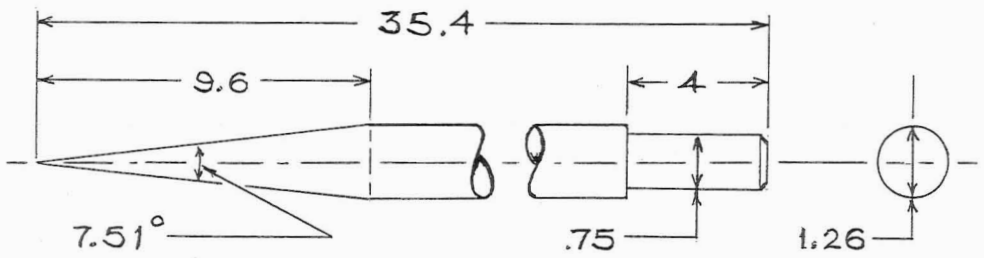

Figure 10. Cone-cylinder test model. Dimensions in inches.

Before the research model pressure signature was measured at each separation distance, the cone-cylinder model was mounted in the test section so that a check pressure signature could be measured and compared with a Whitham theory prediction. In figure 11, a sample set of measured and predicted pressure signatures are presented.

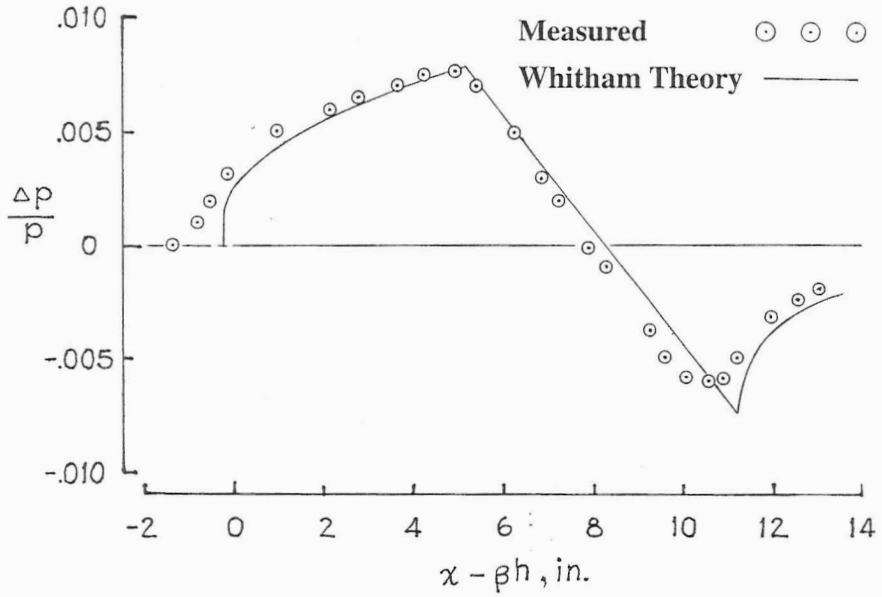

Figure 11. Measured and predicted cone-cylinder pressure signatures. M = 2, and h = 88.9 inches.

Agreement between theory and experiment was acceptably good. Similar agreement was found at the other separation distances. The agreement shown in the two measured pressure signatures, figure 9, and in the measured and predicted pressure signatures, figure 11, was the basis for the decision to measure the pressure signature from the SLSLE model at each separation distance.

Theory And Experiment Comparisons

Three pressure signature characteristics were to be evaluated to determine, or at least estimate, the "limiting" separation distance required for credible extrapolation. The first characteristic was nose shock strength which was analyzed by comparing measured and predicted values across the wind-tunnel test h/b range of 2 to 20 . Second, pressure signature "impulse", i.e. the integral of overpressure along the positive part of the pressure signature, was analyzed by comparing measured and predicted values across the same range. Third, changes in pressure signature shape were

to be analyzed by comparing measured and predicted pressure signatures from the wind-tunnel models at the lift ratio, $C_L / C_{L,CRUISE}$, of 1.0 across the h/b range of 2 to 20 .

Nose Shock Comparisons

Flow field shocks measured in the wind-tunnel test section were rounded instead of sharply abrupt. The nose shock data points were spread over a finite distance because of: (1) finite-sized orifices on the conical survey and reference probes; (2) acoustic propagation in the probe's boundary layer; and (3) model vibration in response to wind-tunnel turbulence. Since they were measured in different test section locations and different wind-tunnel facilities, they also had to be adjusted for real-flow effects and corrected for wind-tunnel test-section effects.

The first adjustment was presented and explained in reference 15. This nose shock adjustment method is demonstrated in figure 12.

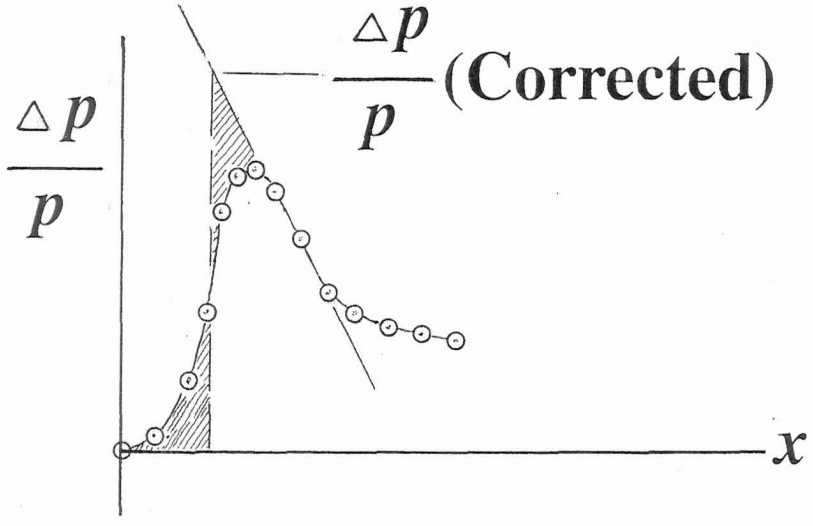

Figure 12. Typical wind-tunnel measured and adjusted nose shock.

Nose shock strength and location was adjusted by "balancing" the shaded areas in the nose-shock region. This permitted credible comparisons between theory and experiment.

A second correction was required because the reference probe static pressures in both tests were different from the test section static pressures defined by Mach number, Reynolds number, total pressure, and total temperature. A derivation of this correction, a list of reference-probe static pressures, and a list test-section static pressures is given in Appendix F.

Corrected nose shock parameters in far-field format, $(\Delta p/p)(h/l_e)^{3/4}$, were obtained for all the pressure signatures measured under the flight path of the models at $C_L / C_{L,CRUISE} = 1.0$. These experimentally derived parameters were compared with theoretical predictions of nose shock parameters at h/b values of 2 to 20 . The usual far-field nose shock parameter was based on the assumption that an N-wave pressure signature had formed and was measured. Low-boom constraints on these research models were set by the desire for the pressure signature to have a "flattop", not an N-wave, shape. So the values used for comparison had near-field magnitudes, and were obtained from theoretical pressure signatures calculated at increasingly large separation distances. Since these models were so similar in overall shape and had the same design goal, a single theory line was used for the comparison presented in figure 13.

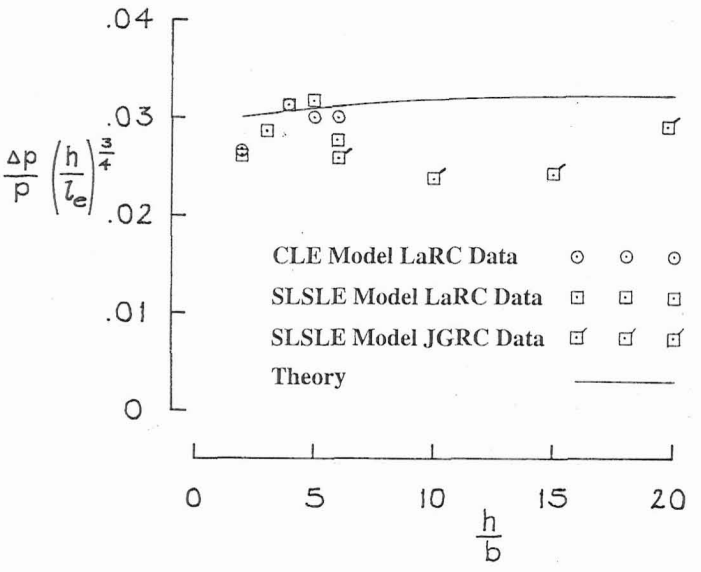

Figure 13. Comparison of corrected and theoretical nose shock parameters versus h / b for both wind-tunnel models. $C_L / C_{L,CRUISE} = 1.0$, and M = 2.

The nose shock overpressure parameter, obtained from measured pressure signatures, should asymptotically approach a far-field value as h / b steadily increases. At the "limiting distance", it should be sufficiently close to the asymptotic value that a credible overpressure prediction could be obtained when a near-field wind-tunnel pressure signature was extrapolated to the ground with the Thomas code. Except for the one SLSLE data point at $h / b = 5$, the adjusted and measured nose shock overpressures obtained in the Langley Facility were "clustered" near an apparent "limiting distance" value at an $h / b = 5$ value.

The nose shock parameter derived from pressure signatures measured at the John Glenn Facility at h / b values from 5 to 20 had a markedly different behavior. All of the measured and adjusted nose shock parameters were grouped about a trend line parallel with, but below, the far-field asymptotic value. The nose shock data points used for the adjustment (shown in figure 12) may have been insufficient for a line or a smooth curve to be passed through them for an impulse balance. The pressure signatures discussed in reference 16 showed a similar trend. N-wave pressure signatures usually had sufficient nose-shock points because the shape was inherently simple, but the low-boom pressure signatures were often not, so some of the calculated nose shock adjustments lacked sufficient precision.

At a nose-shock magnitude less than the asymptotic value, the extended John Glenn Facility nose shock parameter tentatively suggested a "limiting" distance might be between 5 and twenty span lengths. Even though not rapidly approaching the far-field trend value, the data obtained over the h / b range of 2 to 20 straddled a trend line that was fairly flat. By itself, therefore, the nose shock data was not conclusive. Obviously, additional impulse and shape data would be needed to narrow the range of determination and prediction.

Impulse Comparisons

Pressure signature impulse data were corrected for static-pressure differences, but did not need adjustments for rounded shocks. Corrected values of the far-field impulse parameter,

$I(h/l_e)^{1/2}$, from the under-the-flight-path measured pressure signatures at h/b values from 2 to 5 in the Langley Facility, and at h/b values from 5 to 20 in the John Glenn Facility, were compared with theory in figure 14.

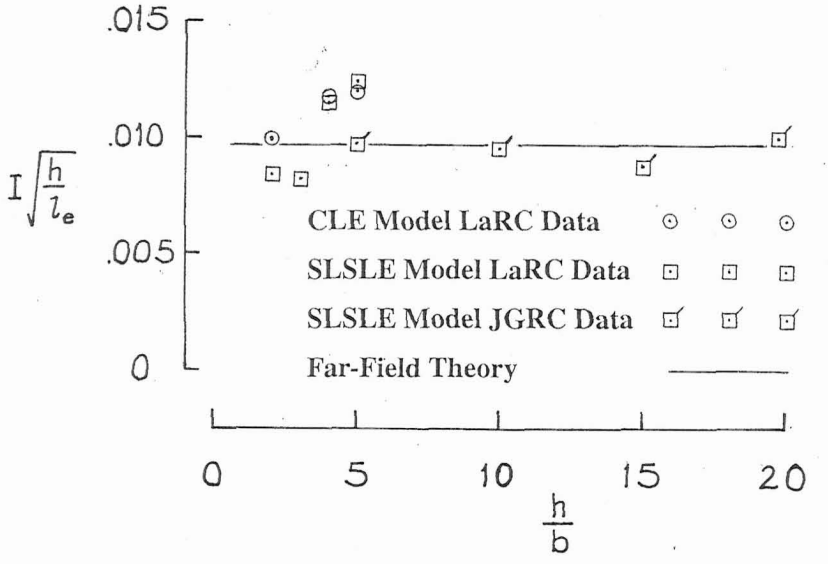

Figure 14. Comparison of theoretical and measured impulse parameter versus h/b for both wind-tunnel models. $C_L / C_{L,CRUISE} = 1.0$, and M = 2.

The impulse values in figure 14, which included data from the Langley Facility and the John Glenn Facility, were expressed with far-field parameters to be consistent with the far-field overpressure parameter plotted in figure 13.

Although the impulse data showed scatter above and below the theoretical lines in the near-field h/b range of 2 to 5, there was much less scatter in the h/b range of 5 to 20. This seemed to suggest that the "limiting distance" value of h/b for credible extrapolation of pressure signatures from the two models would be larger than 5 or 10, but most likely not as large as 20 .

Pressure Signature Shape

The third pressure signature characteristic to be considered in this analysis was the shape of the measured pressure signature, and how it changed, evolved, or "aged" with increasing separation distance. Once beyond a "limiting distance", the low-boom shape should change very little from "limiting distance" to the ground when plotted in the far-field parameters of:

$$(\Delta p/p)(h/l_e)^{3/4} \quad \text{versus} \quad [(x-\beta h)/l_e](h/l_e)^{1/4}$$

Such a pressure signature could be credibly extrapolated to the ground with the Standard Atmosphere Propagation version of the Thomas Code. The Model C pressure signatures, measured at M = 2 and $C_L = 0.10$ in reference 17, displayed this type of behavior at the larger separation distance h/b ratios used in that wind-tunnel study. This certainly was true for both the N-wave and "quasi-shaped" pressure signatures presented in reference 17, so it should also be true for low-boom pressure signatures since atmospheric "freezing", reference 3, would maintain the low-boom shape from this "limiting distance" to the ground.

The closest and the farthest under-the-flight-path separation distances for obtaining complete

signatures in both the Langley Facility and the John Glenn Facility were 9.0 and 88.9 inches respectively, h / b values from 2 to about 20 . Since report-quality pressure signatures from the CLE model were measured only at the Langley Facility and none at the John Glenn Facility, only the pressure signature shape data from the SLSLE model is presented and discussed in the following sections.

Flight-track pressure signatures, generated by the SLSLE model and measured in the Langley Facility at separation distances of 9.0, 13.5, 18.0, and 22.5 inches, are shown in figure 15.

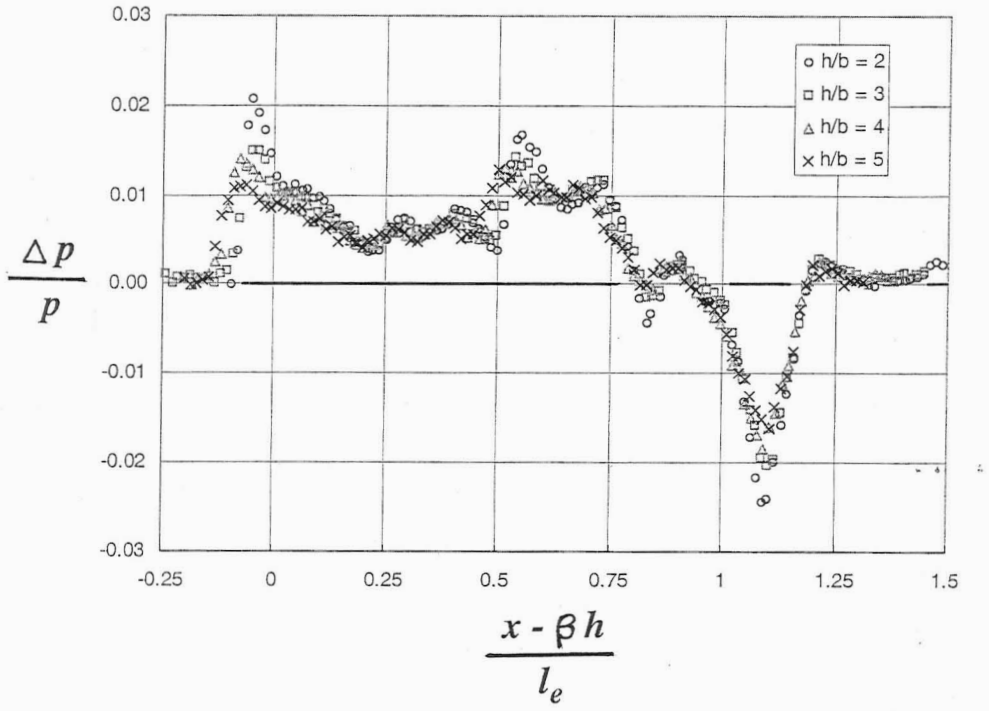

Figure 15. SLSLE model at M = 2, $C_L / C_{L,CRUISE} = 1.0$, h = 9.0, 13.5, 18.0, and 22.5 inches.

A definite change in pressure signature shape was evident in figure 15 as separation distances increased. Nose shock pressure rises became smaller and less peaked, lift-induced pressure rises were more gradual and of lower magnitudes, and the pressure signature lengths increased. Most noticeable was the change in the top of the pressure signature which had slowly settled down into a "flatter" ensemble of positive pressure data points. While these trends were evident and encouraging, it was obvious that more measured pressure signature data, obtained at larger separation distances, were needed before definitive report-goal conclusions could be made.

Pressure signature data from the SLSLE model was measured at the John Glenn Facility at separation distances of 22.5, 45.0, 67.5, and 88.9 inches. (Due to test section equipment and flow constraints, a separation distance of exactly 90 inches was not possible.) Since the pressure signatures measured at a distance of 22.5 inches have already been shown in figures 9 and 15, only the pressure signatures measured at the farther distances of 45.0, 67.5, and 88.9 inches are shown and compared with Whitham theory predictions in figures 16 to 18.

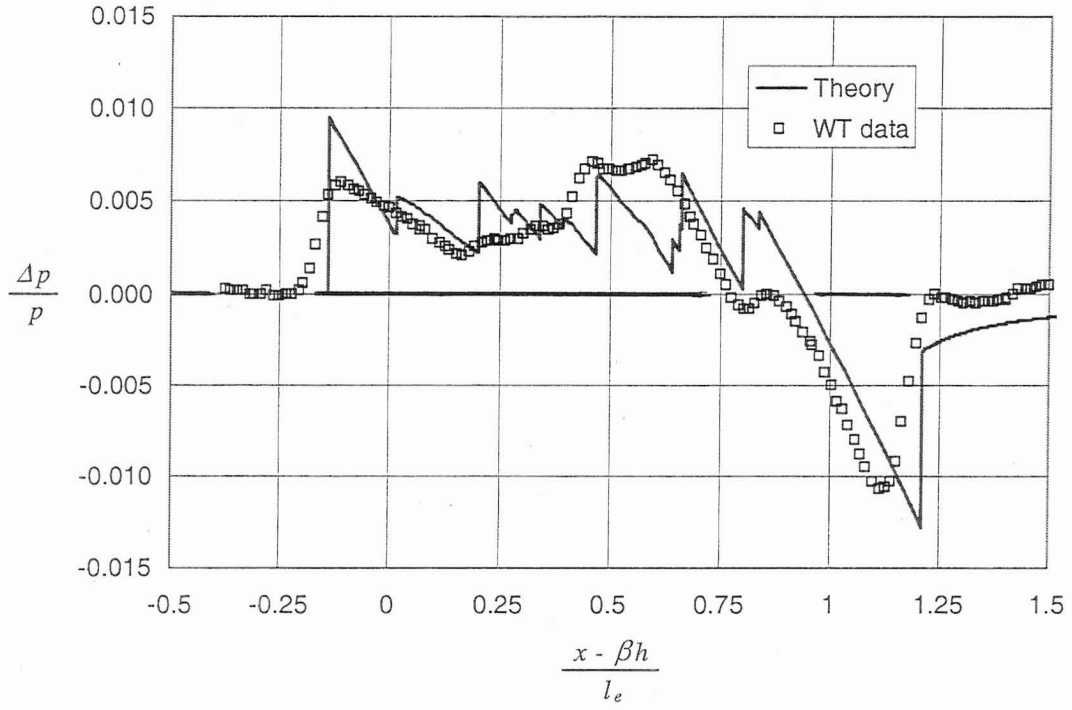

Figure 16. SLSLE model at M = 2, $C_L / C_{L,CRUISE} = 1.0$, and $h = 45.0$ inches.

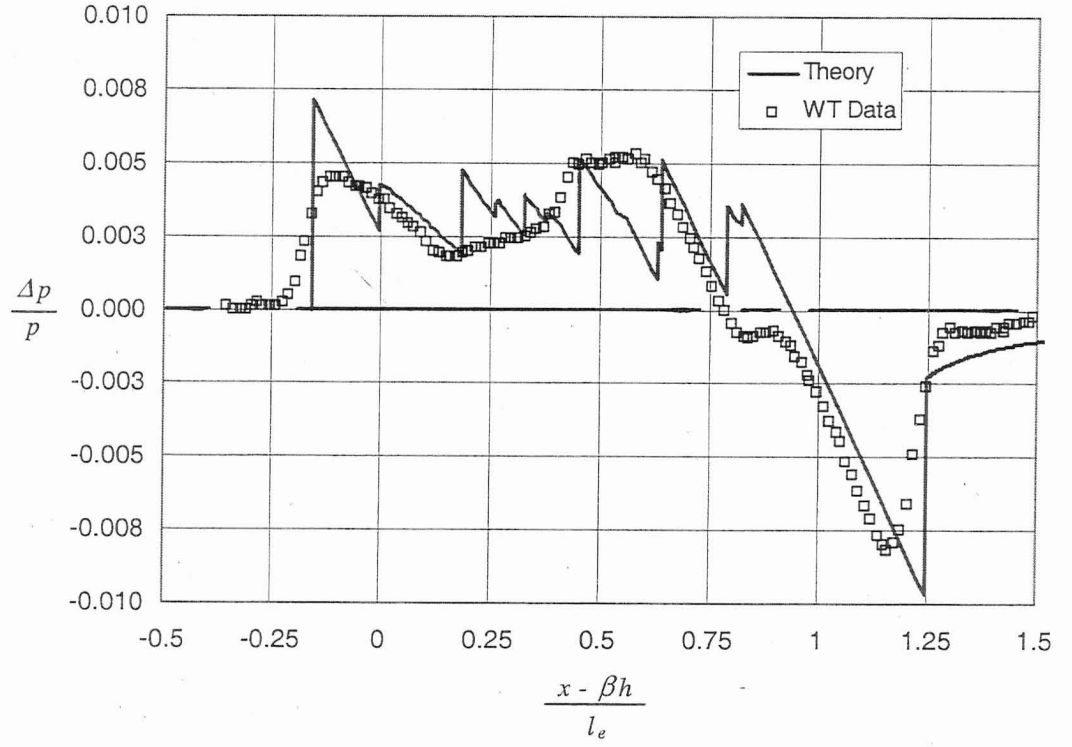

Figure 17. SLSLE model at M = 2, $C_L / C_{L,CRUISE} = 1.0$, and $h = 67.5$ inches.

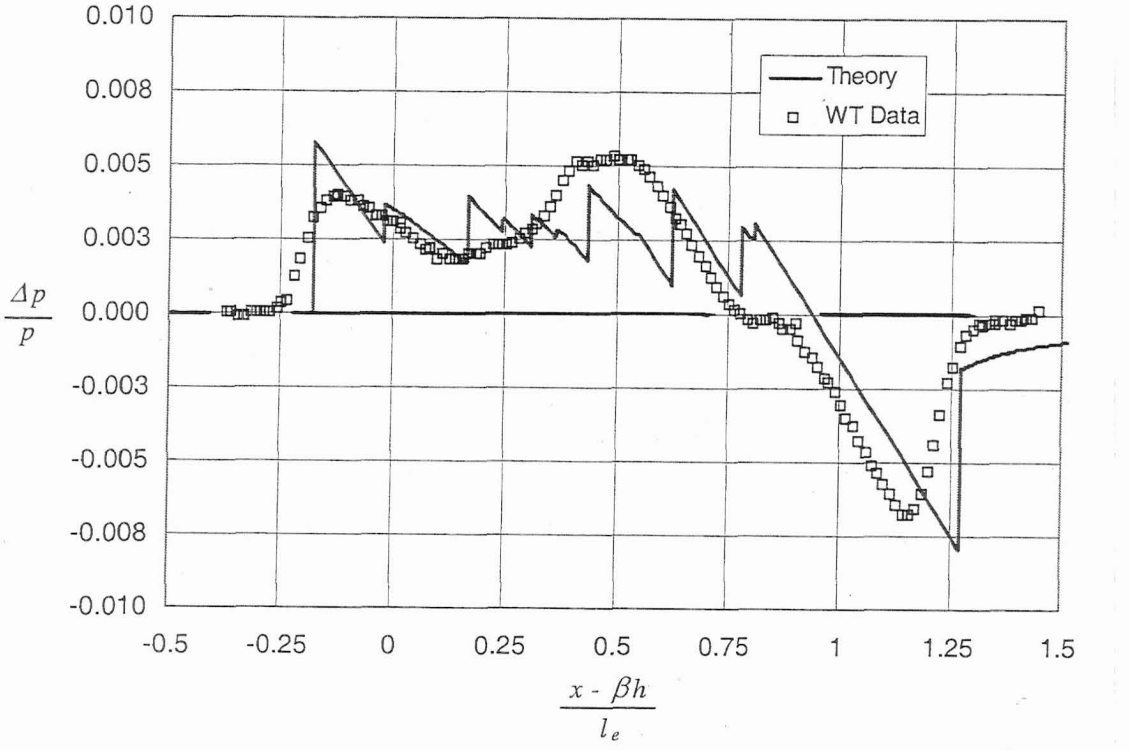

Figure 18. SLSLE model at M = 2, $C_L / C_{L,CRUISE} = 1.0$, and h = 88.9 inches.

Agreement between the Whitham theory predicted and the wind-tunnel measured pressure signatures improved as the separation distance increased from 45.0 to 88.9 inches. Since the Whitham theory was inherently far-field, the good agreement between the theoretical prediction and wind-tunnel measurement at 88.9 inches (distance/span ratio, $h / b = 19.76$) strongly suggested that the separation distances used in this wind-tunnel study had reached and probably extended beyond, the "limiting" extrapolation distance where the application of a pressure signature extrapolation code would be appropriate and provide credible predictions of ground pressure signatures. Since both the Whitham theory and the method employed to write the Thomas Extrapolation code were derived from two-dimensional, first-order, cylindrical propagation models, both would provide similar, but not necessarily the same predictions of shape and magnitudes in a ground overpressure signature.

The evolution, or "aging", of the pressure signature was readily seen by noting changes in measured pressure signature shape as the separation distance increased from 9.0 to 88.9 inches. Three of the seven measured pressure signatures - those measured at increasing separation distances of 9.0, 45.0, and 88.9 inches (h / b = 2.0, 10.0, and 19.76) - were superimposed in figure 19 to quantitatively and qualitatively demonstrate this evolution of pressure signature shape.

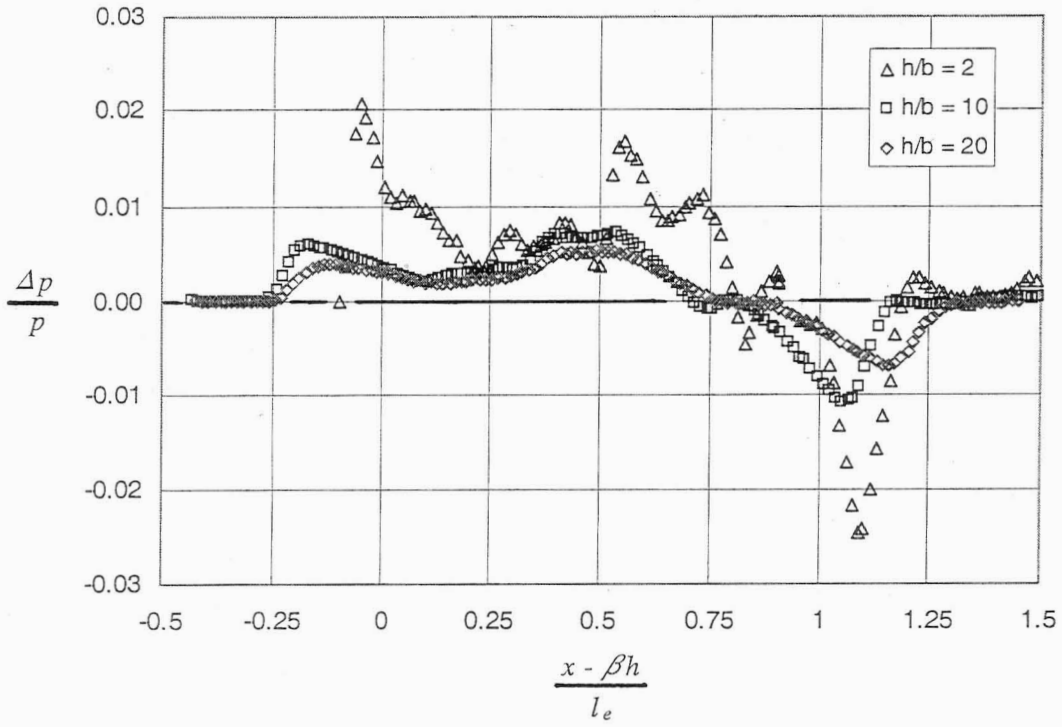

Figure 19. SLSLE model at M = 2, C_L / $C_{L,CRUISE}$ = 1.0, and h/b = 2, 10, and 19.76 .

The pressure signature at a distance ratio of h/b = 19.76 was longer than those at distance ratios of 2 and 10 due to "aging", i.e. spreading and attenuation. The nose and tail shock strengths on the pressure signatures measured at h/b = 10 and 19.76 also showed marked reductions as separation distanced increased. These were the obvious and expected changes.

The most noticeable and most significant observed change in pressure signature shape was that overpressure disturbances along the positive section of the measured pressure signatures became leveler and smoother as the separation distances increased. Mini-shocks along the positive section of the measured pressure signature at the closest separation had attenuated in strength, but had not showed any tendency to move forward to coalesce with the nose shock as the separation distance increased. On the ground, the pressure signature would probably have the low-boom shape shown in figure 4(b) which is very close to the desired shape. The observed changes in the shape of pressure signature shown in figure 19 as well as the favorable agreement between Whitham Theory predictions and the measured pressured pressure signatures seen in figures 16 to 18 prompted the conclusion that a "limiting" distance for extrapolation of these wind-tunnel measured pressure signatures could be found within the range of 15 and 20 span lengths.

The CLE model's pressure signatures, measured at separation distances of 9, 18.0, and 22.5 inches (h/b = 2, 4, and 5), reference 6, were very similar to those generated by the SLSLE model at the same separation distances. Thus, the same favorable conclusions about reaching a limiting distance could be obtained based on the predicted pressure signatures from the CLE concept, figure 4(a), and the measured pressure signatures from its model, even though they were obtained over a shorter range of separation distances.

Discussion

Three analytic methods were employed to determine a limiting distance for the credible extrapolation of near-field pressure signatures from cruise altitude to the ground. The first method was an analysis of nose shock strength attenuation with increasing separation distance. While relatively easy to perform, it proved to be the least useful of the three methods. There were an insufficient number of good data points available at the larger separation distances for an accurate estimation of adjusted nose shock strength.

The second method was an analysis of the change in pressure signature impulse with increasing separation distance. This method, which depended on the integration of overpressures in the positive section of the pressure signature, resulted in trend information which helped narrow the range of possible limiting distances from the full range of separation distances used during the measurement of pressure signature at the two wind-tunnel facilities.

The third method was a qualitative evaluation of the change in pressure signature shape as separation distance increased. Pressure signature shapes and features that changed as separation distances increased corroborated trends observed and identified during the application of methods one and two, especially those seen with method two.

It was not too surprising that the ideal "flattop" pressure signature shapes were not achieved at the near-field separation distances available in the Langley Facility test section. The strongly three dimensional lift effects that created doublet-like disturbances were larger and far more influential than the volume effects on both models. Additional data obtained at the John Glenn Research Center, however, demonstrated the additional pressure signatures, measured at the extended separation distances in a larger wind-tunnel test section, i.e. distances corresponding to h / b ratios of 5 to 20, definitely had been required. Results obtained from the application of the three pressure signature evaluation methods to the measured wind-tunnel obtained from both facilities indicated that a limiting distance for extrapolation had been achieved at

$$15 < (h/b)_{\text{LIMITING}} < 20$$

This conclusion was based on comparisons of the measured pressure signatures with Whitham theory predictions, figures 15 through 18, and the shapes of the two pressure signatures measured at 2, 10, and 20 span lengths, figure 19.

These results were in good agreement with a preliminary data analysis presented in reference 18. The wind-tunnel data in that report showed that a wind-tunnel model designed with low-boom tailoring might need separation distances of more than 4 to 5 span lengths before the measured pressure signatures began to show strong tendencies toward attaining and keeping a low-boom shape. However, that same report, based on reference 17, showed that a configuration with approximate low-boom tailoring also generated pressure signatures with near-field shape features that persisted over very long distances.

An empirical study done with the theoretical and experimental data in reference 19 provided two parallel methods for estimating a limiting extrapolation distance. Using the two derived equations, one based on geometric acoustics and the other on overpressure impulse ratios, an upper and lower value of $(h / b)_{\text{LIMITING}}$ was predicted to be:

$$16 < (h/b)_{\text{LIMITING}} < 17$$

This prediction corroborated and narrowed the limiting distance range estimated from the measured wind-tunnel pressured signature data presented in this report.

A previous empirical study, reference 20, established the groundwork for the predictions presented in reference 19. Based on a reworking of equation (4) in reference 20, it provided a very conservative prediction of:

$$(h/b)_{\text{LIMITING}} = 16 \text{ (approximately)}$$

This prediction was less than the outer separation distance, and well within the range of separation distances used in the current wind-tunnel study. Because a more detailed acoustic propagation model was used in reference 19, the predictions from that source seemed more reasonable even though they were more conservative. However, all the values of $(h/b)_{\text{LIMITING}}$, predicted by these various methods, were considerably greater than the 0.5 to 2.0 (h/b) values employed by previous researchers (references 21 to 23 are typical) extrapolating CFD-calculated and wind-tunnel-measured near-field pressure signatures to the ground with the Thomas Code. Since all the conclusions and predictions presented in this paper were obtained from a limited set of wind-tunnel data, and from an empirical modeling of near-field physics, more pressure signature measurements obtained over a similar range of separation distance ratios with other low-boom models seems to be warranted.

Since the CLE model could not provide credible pressure signature data at the larger separation distances available in the John Glenn Facility, the question of the effect of the wing's leading edge shape on the ease of achieving low-boom ground overpressures remained unanswered. The results obtained in the Langley Facility at the smaller separation distances suggested, but did not indicate, a smooth and continuous leading edge would provide benefits from a slightly lower impulse value, but there was not enough pressure signature data for definite conclusions. In theory, the curved smooth and continuous leading edge would be preferred. In practice, however, the difference in low-boom performance between a concept with a curved leading edge and a concept with a well-crafted straight-line segmented leading edge may be too small for serious concern.

Concluding Remarks

A two-part study was conducted at the Langley and John Glenn Research Centers to determine: (1) a limiting distance for the extrapolation of pressure signatures to the ground, and (2) the effect of wing leading edge shape on low-boom performance. An analysis of data obtained at the Langley Research Center indicated pressure signatures did not develop the desired "flattop" shape features in the available 2 to 5 span length near-field region of the Langley Unitary Plan wind-tunnel test section. However, the measured pressure signatures were starting to acquire "flattopp" features at the maximum separation distance of 5 span lengths. This trend toward the "flattop" pressure signature was not strong, but it was consistent with results seen before in previous wind-tunnel measurements of near-field pressure signatures from other models with geometries tailored to generate low-boom shaped pressure signatures on the ground.

At the John Glenn Research Center, only the Straight-Line-Segmented Leading Edge Model was used to obtain measured pressure signatures at the two $C_L / C_{L,CRUISE}$ ratios and in the larger separation distance ratio range of 5 to 20. A defective temperature compensator in the strain gauge circuit of the Curved Leading Edge Model's lift-moment balance made it impossible to obtain valid pressure signatures at any of the desired separation distances. So this model was withdrawn from the test program.

An analysis of the Straight-Line-Segmented Leading Edge Model pressure signatures measured at separation distances of 22.5, 45.0, 67.5, and 88.9 inches (5, 10, 15, and 19.76 span lengths) showed definite indications that these signatures had attenuated and "aged" sufficiently to show limiting distance shape characteristics. From these results, an estimate of a minimum extrapolation distance in the range of 15 to 20 span lengths along the flight track below the model was determined. A prediction based on a previously reported empirical method narrowed this range down to about 16 to 17 span lengths. This predicted limiting extrapolation distance range was 10 to 20 times larger than the span length distances used previously to obtain extrapolated ground pressure signatures from CFD-calculated or wind-tunnel-measured input data.

Pressure signature data was obtained with the Curved Leading Edge Model and the Straight-Line-Segmented Leading Edge Model at the Langley Facility in the range of 2 to 5 span lengths. Impulse and nose shock calculations performed at this distance-to-span ratio range indicated there might be a small low-boom benefit obtained with the use of a smoothly continuous wing leading edge. However, no corroborating pressure signature data was obtained at the larger separation distances with the Curved Leading Edge Model at the John Glenn Facility. So, there were no conclusive pressure signature data to support definite conclusions about the benefits of a curved leading edge versus a straight-line segmented leading edge.

References

1. Thomas, Charles L.: *Extrapolation Of Sonic Boom Pressure Signatures By The Wave Form Parameter Method.* NASA TN D-6832, 1972.

2. Hicks, Raymond M.; and Mendoza, Joel P.: *Prediction Of Aircraft Sonic Boom Characteristics From Experimental Near Field Results.* NASA TM X-1477, September 1967.

3. Hayes, Wallace D.; Haefeli, Rudolph C.; and Kulsrud, H. E.: *Sonic Boom Propagation In A Stratified Atmosphere, With Computer Program.* NASA CR-1299, 1969.

4. Whitham, G. B.: *The Flow Pattern of a Supersonic Projectile.* Communications on Pure and Applied Mathematics vol. V, no. 3, August 1952, pp. 301-348.

5. Walkden, F.: *The Shock Pattern of a Wing-Body Combination, Far From the Flight Path.* Aeronautical Quarterly, vol. IX, pt. 2, May 1958, pp. 164-194.

6. Mack, Robert J.; and Kuhn, Neil S.: *Determination Of Extrapolation Distance With Measured Pressure Signatures From Two Low-Boom Models.* NASA / TM-2004-213264, November 2004

7. Mack, Robert J.: *A Supersonic-Cruise Business Jet Concept Designed For Low Sonic Boom.* NASA / TM-2003-212435, October 2003

8. Mack, Robert J.; and Haglund, George T.: *A Practical Low-Boom Overpressure Signature Based On Minimum Sonic Boom Theory.* High-Speed Research: Sonic Boom, Volume II, NASA Conference Publication 3173, 1992.

9. Seebass, R.; and George, A. R.: *Sonic-Boom Minimization.* Journal of the Acoustical Society of America, vol. 51, no. 2, pt. 3, February 1972, pp. 686 - 694.

10. Darden, Christine M.: *Sonic Boom Minimization With Nose-Bluntness Relaxation.* NASA TP-1348, 1979.

11. Carlson, Harry W.; Barger, Raymond L.; and Mack, Robert J.: *Application Of Sonic-Boom Minimization Concepts In Supersonic Transport Design.* NASA TN D-7218, June 1973.

12. Mack, Robert J.; and Darden, Christine M.: *Wind-Tunnel Investigation Of The Validity Of A Sonic-Boom-Minimization Concept.* NASA TP-1421, 1979.

13. Harris, Roy V., Jr.: *A Numerical Technique For Analysis Of Wave Drag At Lifting Conditions.* NASA TN D-3586, 1966.

14. Craidon, Charlotte B.: *Description Of A Digital Computer Program For Airplane Configuration Plots.* NASA TM X-2074, 1970.

15. Carlson, Harry W.: *Correlation Of Sonic-Boom Theory With Wind-Tunnel And Flight Measurements.* NASA TR R-213, December 1964.

16. Carlson, Harry W.; Mack, Robert J.; and Morris, Odell A.: *A Wind-Tunnel Investigation Of The Effect Of Body Shape On Sonic-Boom Pressure Distributions.* NASA TN D-3106, November 1965.

17. Morris, Odell A.: *A Wind-Tunnel Investigation At A Mach Number Of 2.01 Of The Sonic-Boom Characteristics Of Three Wing-Body Combinations Differing In Wing Longitudinal Location.* NASA TN D-1384, September 1962.

18. Mack, Robert J.: *Persistence Characteristics of Wind-Tunnel Pressure Signatures From Two Similar Models.* NASA/TM-2004-212671, January 2004.

19. Mack, Robert J.: *Anomalous Shocks On The Measured Near-Field Pressure Signatures Of Low-Boom Wind-Tunnel Models.* NASA/TM-2006-214496, August 2006.

20. Mack, Robert J.; and Darden, Christine M.: *Limitations On Wind-Tunnel Pressure Signature Extrapolation.* High-Speed Research: Sonic Boom, Volume II, NASA Conference Publication 3173, February 1992.

21. Fouladi, Kamran; and Baize, Daniel: *CFD Predictions of Near-Field Pressure Signatures of a Low-Boom Aircraft.* High-Speed Research: Sonic Boom, Volume II, NASA Conference Publication 3173, February 1992.

22. Plotkin, Kenneth K.; and Page, Juliet A.: *Extrapolation of Sonic Boom Signatures From CFD Solutions.* AIAA 2002-0922

23. Morgenstern, John M.: *Wind Tunnel Testing of a Sonic Boom Minimized Tail-Braced Wing Transport Configuration.* AIAA 2004-4536

Appendix A

Brief Description of Two Low-Boom Wind-Tunnel Models and Concepts

	SLSLE Model	CLE Model
Span, in	4.5	4.5
Effective Length, in	9.0	9.0
Lift Length, in	9.0	9.0
Wing Area, in^2	10.08	10.0737
Mean Aerodynamic Chord, in	2.9615	2.9728
Aspect Ratio, b^2/S	2.0	2.0

The following flight data pertains to the full-scale wing / fuselage concepts.

	SLSLE Concept	CLE Concept
Cruise Altitude, ft	53,000.0	53,000.0
Beginning Cruise Weight, lb	88,000.0	88,000.0
Beginning Cruise Wing Loading, psf	49.386	49.386
Beginning Cruise C_L	0.08309	0.08309
Cruise Mach Number	2.0	2.0
Ground-Level Overpressure, psf	0.50	0.50
Ground-Level Reflection Factor	1.90	1.90
Type of Overpressure Shape	"Flattop"	"Flattop"

The two low-boom wind-tunnel models, used to measure pressure signatures, were 1:160 versions of the full-scale concepts, with the aft fuselage modified to blend smoothly into the cylindrical sting. Numerical descriptions of the two low-boom wind-tunnel models are listed in Wave Drag format, references 13 and 14, in Appendix B and Appendix C.

Appendix B

Numerical Description Of The Curved Leading-Edge Concept
(Lengths in ft, areas in ft^2)

```
Curved Leading Edge Wing Model, Flat Wing, Cambered Fuselage
  1  1 -1  0  0  0  0  9 17  3 19 30 19 30 19 10
1790.88                                                                                                  REF AREA
0.0     2.5     5.0     10.0    15.0    20.0    30.0    40.0    50.0    60.0                            X AF 1
70.0    80.0    85.0    90.0    95.0    97.5    100.0                                                   X AF 2
46.561 3.50    -.4867 55.7722                                                                           WAFORG1
62.800 7.20    -.6226 42.0000                                                                           WAFORG2
70.000 9.20    -.6639 36.1333                                                                           WAFORG3
75.200 11.2    -.6171 32.2667                                                                           WAFORG4
80.000 13.2    -.5528 28.8000                                                                           WAFORG5
86.000 16.0    -.4311 24.6667                                                                           WAFORG6
112.40 29.2     0.2258 7.06667                                                                          WAFORG7
113.60 29.6     0.2281 6.13333                                                                          WAFORG8
116.00 30.0     0.1776 4.00000                                                                          WAFORG9
0.0     -.0619  -.1238  -.2476  -.3714  -.4953  -.7429  -.9905  -1.238  -1.486                         ZORD1
-1.733  -1.981  -2.105  -2.229  -2.352  -2.414  -2.476                                                 ZORD1
0.0     -.0466  -.0932  -.1865  -.2797  -.3730  -.5594  -.7459  -.9324  -1.119                         ZORD2
-1.305  -1.492  -1.585  -1.678  -1.772  -1.818  -1.865                                                 ZORD2
0.0     -.0401  -.0802  -.1604  -.2406  -.3209  -.4813  -.6417  -.8022  -.9626                         ZORD3
-1.123  -1.283  -1.364  -1.444  -1.524  -1.564  -1.604                                                 ZORD3
0.0     -.0358  -.0716  -.1433  -.2149  -.2865  -.4298  -.5731  -.7163  -.8596                         ZORD4
-1.003  -1.146  -1.218  -1.289  -1.361  -1.397  -1.433                                                 ZORD4
0.0     -.0320  -.0640  -.1278  -.1918  -.2557  -.3836  -.5115  -.6394  -.7672                         ZORD5
-.8951  -1.023  -1.087  -1.151  -1.215  -1.247  -1.279                                                 ZORD5
0.0     -.0274  -.0548  -.1095  -.1643  -.2190  -.3286  -.4381  -.5476  -.6571                         ZORD6
-.7666  -.8762  -.9309  -.9857  -1.040  -1.068  -1.095                                                 ZORD6
0.0     -.0078  -.0157  -.0314  -.0471  -.0628  -.0941  -.1255  -.1569  -.1883                         ZORD7
-.2196  -.2510  -.2667  -.2823  -.2981  -.3059  -.3138                                                 ZORD7
0.0     -.0068  -.0136  -.0272  -.0408  -.0545  -.0817  -.1089  -.1362  -.1634                         ZORD8
-.1906  -.2179  -.2315  -.2451  -.2587  -.2655  -.2723                                                 ZORD8
0.0     -.0044  -.0089  -.0178  -.0266  -.0355  -.0533  -.0710  -.0888  -.1066                         ZORD9
-.1243  -.1421  -.1510  -.1598  -.1687  -.1732  -.1776                                                 ZORD9
0.0     .1560   .3040   .5760   .8160   1.024   1.344   1.536   1.600   1.536                         WAF1
1.344   1.024   .8160   .5760   .3040   .1560   0.0                                                    WAF1
0.0     .1560   .3040   .5760   .8160   1.024   1.344   1.536   1.600   1.536                         WAF2
1.344   1.024   .8160   .5760   .3040   .1560   0.0                                                    WAF2
0.0     .1560   .3040   .5760   .8160   1.024   1.344   1.536   1.600   1.536                         WAF3
1.344   1.024   .8160   .5760   .3040   .1560   0.0                                                    WAF3
0.0     .1560   .3040   .5760   .8160   1.024   1.344   1.536   1.600   1.536                         WAF4
1.344   1.024   .8160   .5760   .3040   .1560   0.0                                                    WAF4
0.0     .1560   .3040   .5760   .8160   1.024   1.344   1.536   1.600   1.536                         WAF5
1.344   1.024   .8160   .5760   .3040   .1560   0.0                                                    WAF5
0.0     .1560   .3040   .5760   .8160   1.024   1.344   1.536   1.600   1.536                         WAF6
1.344   1.024   .8160   .5760   .3040   .1560   0.0                                                    WAF6
0.0     .1560   .3040   .5760   .8160   1.024   1.344   1.536   1.600   1.536                         WAF7
1.344   1.024   .8160   .5760   .3040   .1560   0.0                                                    WAF7
0.0     .1560   .3040   .5760   .8160   1.024   1.344   1.536   1.600   1.536                         WAF8
1.344   1.024   .8160   .5760   .3040   .1560   0.0                                                    WAF8
0.0     .1560   .3040   .5760   .8160   1.024   1.344   1.536   1.600   1.536                         WAF9
1.344   1.024   .8160   .5760   .3040   .1560   0.0                                                    WAF9
0.0     1.0     2.0     3.0     4.0     5.0     6.0     7.0     8.0     9.0                           X FUSE1
10.0    12.0    14.0    16.0    18.0    20.0    22.5    25.0    27.5    30.0                          X FUSE2
32.50   35.00   37.50   40.00   42.50   45.00   47.50   50.00   52.50   55.00                         X FUSE3
0.0     0.0     0.0     0.0     0.0     0.0     0.0     0.0     0.0     0.0                           Z FUS1
0.0     0.0     0.0     0.0     0.0     0.0     0.0     0.0     0.0     0.0                           Z FUS2
-.0125  -.05    -.1125  -.2     -.308   -.418   -.528   -.638   -.748   -.858                         Z FUS3
0.0     .18247  .72988  1.6490  2.9316  4.6568  6.3794  7.7191  8.8141  9.8145                        FUS AREA1
10.869  12.819  14.780  16.763  18.781  20.718  23.157  25.518  28.086  30.339                        FUS AREA2
32.271  34.108  35.891  37.719  39.258  40.942  42.545  43.826  44.651  45.365                        FUS AREA3
55.00   57.50   60.00   62.50   65.00   67.50   70.00   72.50   75.00   77.50                         X FUS4
80.00   82.50   85.00   87.50   90.00   92.50   95.00   97.50   100.0   102.5                         X FUS5
105.0   107.5   110.0   112.5   115.0   117.5   120.0   122.5   125.0   127.5                         X FUS6
-.858   -.968   -1.078  -1.188  -1.298  -1.408  -1.518  -1.628  -1.738  -1.848                        Z FUS4
-1.958  -2.068  -2.178  -2.288  -2.398  -2.508  -2.618  -2.728  -2.838  -2.948                        Z FUS5
-3.058  -3.168  -3.278  -3.388  -3.498  -3.608  -3.718  -3.828  -3.938  -4.048                        Z FUS6
45.365  45.365  45.365  44.651  44.226  43.179  41.854  40.264  38.265  35.944                        FUS AREA4
33.336  30.288  26.970  23.243  19.494  15.834  12.378  10.010  8.8141  8.5530                        FUS AREA5
8.5530  8.5530  8.5530  8.5530  8.5530  8.5530  8.5530  8.5530  8.5530  8.5530                        FUS AREA6
127.5   130.0   132.5   135.0   137.5   140.0   142.5   145.0   147.5   149.857                       X FUS7
-4.048  -4.158  -4.268  -4.378  -4.488  -4.598  -4.708  -4.818  -4.928  -5.0317                       Z FUS7
8.5530  8.5530  8.5530  8.5530  8.5530  8.5530  8.5530  8.5530  8.5530  8.5530                        FUS AREA7
   12000  96   24   2                    000                                                          AOA
32.0    80.00                                                                                        XREST
```

Appendix C

Numerical Description Of The Straight-Line-Segment Leading-Edge Concept
(Lengths in ft, Areas in ft^2)

```
Straight Line Segmented Leading Edge Wing Model, Flat Wing, Cambered Fuselage
  1  1 -1  0  0  0  0  4 17  3 19 30 19 30 19  9
1792.00                                                                  REF AREA
0.0     2.5     5.0     10.0    15.0    20.0    30.0    40.0    50.0    60.0     X AF 1
70.0    80.0    85.0    90.0    95.0    97.5    100.0                            X AF 2
42.2    3.25    -.0990 59.9666                                                   WAFORG1
66.00   8.00    -.5548 39.3333                                                   WAFORG2
82.00   14.0    -.4867 27.3333                                                   WAFORG3
114.0   30.0    0.1831 6.00000                                                   WAFORG4
0.0     -0.0643-0.1286-0.2571-0.3857-0.5142-0.7713-1.0284-1.2855-1.5427  ZORD1
-1.7998-2.0569-2.1854-2.3140-2.4425-2.5068-2.5711
0.0     -0.0422-0.0843-0.1686-0.2530-0.3373-0.5059-0.6746-0.8432-1.0119  ZORD2
-1.1805-1.3491-1.4335-1.5178-1.6021-1.6443-1.6864
0.0     -0.0293-0.0586-0.1172-0.1758-0.2344-0.3516-0.4688-0.5860-0.7032  ZORD3
-0.8203-0.9375-0.9961-1.0547-1.1133-1.1426-1.1719
0.0     -0.0064-0.0129-0.0257-0.0386-0.0515-0.0772-0.1029-0.1286-0.1544  ZORD4
-0.1801-0.2058-0.2187-0.2315-0.2444-0.2508-0.2573
0.0     .1560   .3040   .5760   .8160   1.024   1.344   1.536   1.600   1.536    WAF1
1.3440  1.024   .8160   .5760   .3040   .1560   0.0                              WAF1
0.0     .1560   .3040   .5760   .8160   1.024   1.344   1.536   1.600   1.536    WAF2
1.3440  1.024   .8160   .5760   .3040   .1560   0.0                              WAF2
0.0     .1560   .3040   .5760   .8160   1.024   1.344   1.536   1.600   1.536    WAF3
1.3440  1.024   .8160   .5760   .3040   .1560   0.0                              WAF3
0.0     .1560   .3040   .5760   .8160   1.024   1.344   1.536   1.600   1.536    WAF4
1.3440  1.024   .8160   .5760   .3040   .1560   0.0                              WAF4
0.0     1.0     2.00    3.00    4.00    5.00    6.00    7.00    8.00    9.00     X FUSE 1
10.0    12.0    14.0    16.0    18.0    20.0    22.5    25.0    27.5    30.0     X FUSE 2
32.50   35.00   37.50   40.00   42.50   45.00   47.50   50.00   52.50   55.00    X FUSE 3
0.0     0.0     0.0     0.0     0.0     0.0     0.0     0.0     0.0     0.0      ZFUS1
0.0     0.0     0.0     0.0     0.0     0.0     0.0     0.0     0.0     0.0      ZFUS2
-.0001  -.0030  -.0150  -.0480  -.1080  -.2152  -.3221  -.4296  -.5368  -.6440   ZFUS3
0.0000  0.1839  0.7355  1.6548  2.9419  4.5968  6.6194  8.1209  9.1201  9.9878   FUS AREA1
10.934  12.888  14.908  16.973  19.065  21.165  23.775  26.340  28.830  31.217   FUS AREA2
33.477  35.586  37.523  39.272  40.814  42.136  43.227  44.076  44.677  45.023   FUS AREA3
55.00   57.50   60.00   62.50   65.00   67.50   70.00   72.50   75.00   77.50    X FUS4
80.00   82.50   85.00   87.50   90.00   92.50   95.00   97.50   100.0   102.5    X FUS5
105.0   107.5   110.0   112.5   115.0   117.5   120.0   122.5   125.0   127.5    X FUS6
-.6440  -.7511  -.8583  -.9655  -1.0727-1.1799-1.2871-1.3943-1.5015-1.6087  Z FUS4
-1.7159-1.8231-1.9302-2.0374-2.1446-2.2518-2.3590-2.4662-2.5734-2.6806  Z FUS5
-2.7878-2.8950-3.0022-3.1094-3.2165-3.3237-3.4309-3.5382-3.6457-3.7525  Z FUS6
45.023  45.119  45.050  44.785  44.125  43.075  41.715  40.059  38.128  35.945   FUS AREA4
33.535  30.931  28.167  25.050  21.350  17.419  14.395  12.400  11.180  10.350   FUS AREA5
9.750   9.350   9.007   8.803   8.703   8.703   8.703   8.703   8.703   8.703    FUS AREA6
127.5   130.0   132.5   135.0   137.5   140.0   142.5   145.0   149.265          X FUS7
-3.7525-3.8597-3.9669-4.0741-4.1813-4.2885-4.3956-4.5028-4.6856                 Z FUS7
8.703   8.703   8.703   8.703   8.703   8.703   8.703   8.703   8.703            FUS AREA7
  12000  96  24   2             000                                              AOA
32.0    80.00                                                                    XREST
```

Appendix D

Langley Research Center Unitary Plan Wind Tunnel Facility

Wind-Tunnel Pressure Signature Measurements

h / b and $C_L / C_{L,CRUISE}$ Values

Distances Under Probe No. 2

h, inches	h / b[1]	$C_L / C_{L,CRUISE}$	Model
9.00	2.00	0.5, 1.0	SLSLE, CLE
13.50	3.00	0.5, 1.0	SLSLE[2]
18.00	4.00	0.5, 1.0	SLSLE, CLE
22.50	5.00	0.5, 1.0	SLSLE, CLE
27.00	6.00	0.5, 1.0	SLSLE, CLE[3]

Off-Track Distances

Probe No. 1 : 2.95 inches to the right of under-the-track Probe No. 2
Probe No. 3 : 6.35 inches to the left of under-the-track Probe No. 2

Off-track distances were measured facing the wind-tunnel throat

The initials CLE represent the model with a Curved Leading Edge that was smoothly continuous.

The initials SLSLE represent the model with a Straight-Line Segmented Leading Edge.

1. The span, b, of both models was 4.5 inches.
2. Pressure signatures generated by the CLE model at a model-No. 2 probe separation distance of 13.5 inches ($h / b = 3.0$) were part of the schedule. However, the track mechanism that moved the three-probe measurement rake became inoperative before the CLE model pressure signature could be measured at $h / b = 3.0$.
3. Only forward section of the pressure signature measured. At this point in the signature measurement, the model noses were already slightly forward of the test section and extended into the aft section of the wind-tunnel nozzle where non-uniform Mach number gradients and flow angularities existed.

Appendix E

John Glenn Research Center Supersonic 10 Foot x 10 Foot Wind Tunnel Facility

Wind-Tunnel Pressure Signature Measurements

h / b and $C_L / C_{L,CRUISE}$ Values

Distances Under Probe No. 1

h, inches	h / b[1]	$C_L / C_{L,CRUISE}$	Model
22.50	5.00	0.5, 1.0	CLE, SLSLE[2]
45.00	10.00	0.5, 1.0	SLSLE[2]
67.50	15.00	0.5, 1.0	SLSLE[2]
90.00	20.00	0.5, 1.0	SLSLE[2]

Off-Track Distances

Probe No. 2 : 18 inches to the right of under-the-track Probe No. 1
Probe No. 3 : 27 inches to the right of under-the-track Probe No. 1

Off-track distances were measured facing the wind-tunnel throat

The initials CLE represent the model with a Curved Leading Edge that was smoothly continuous.

The initials SLSLE represent the model with a Straight-Line Segmented Leading Edge.

1. The span, *b*, of both models was 4.5 inches.
2. Pressure signatures from the CLE model were measured at the John Glenn Research Center Supersonic Wind Tunnel Facility, but could not be used for this report. A failure of the temperature-compensation section of the strain gauges measuring normal force and pitching moment was discovered during initial measurements of pressure signatures at a separation distance of 22.5 inches. This failure was confirmed during a thorough calibration of the CLE model's strain-gauge balance once it was taken from the wind-tunnel test section.

Appendix F

Test-Section Static Pressure Corrections

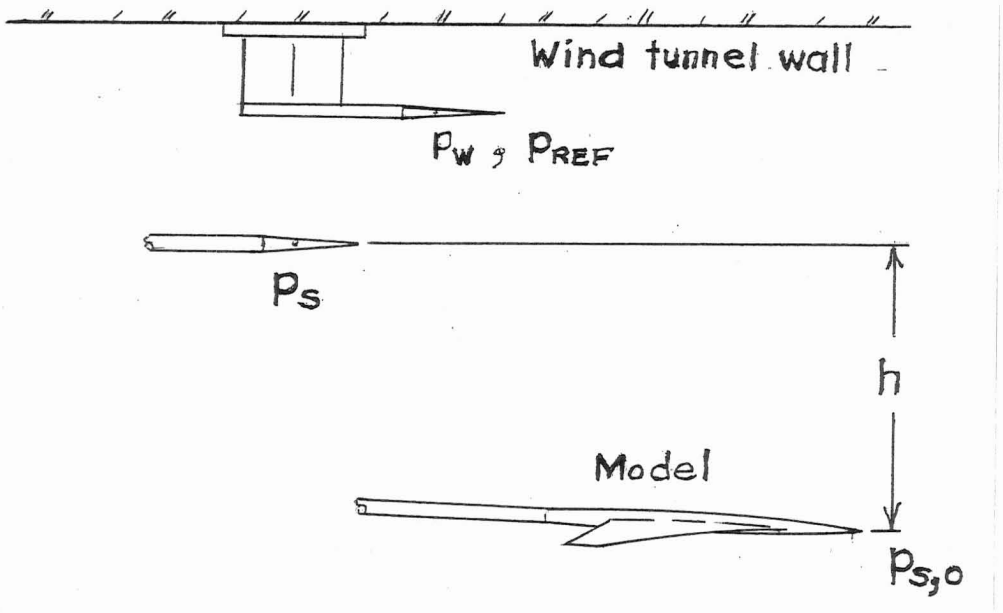

Figure F1. Typical model, survey probe, reference probe in wind-tunnel test section.

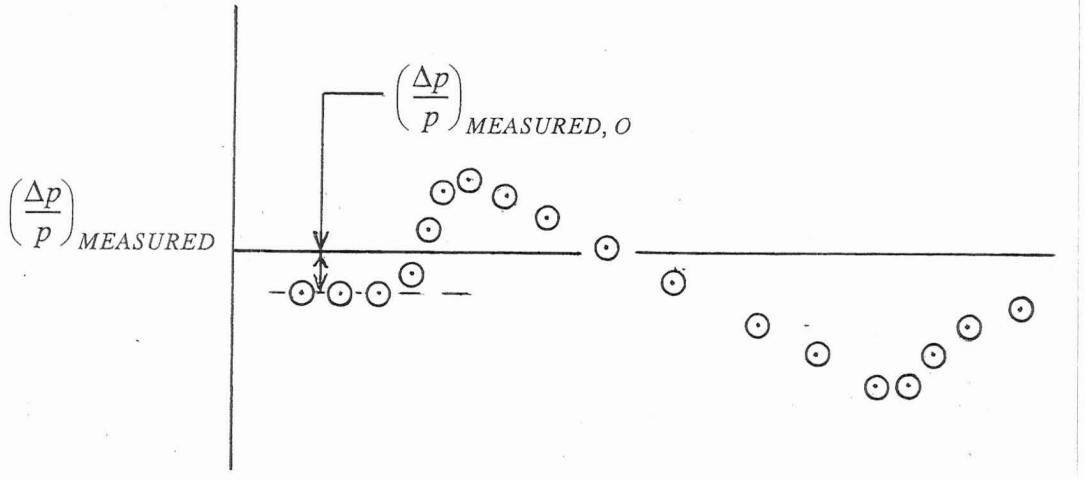

Figure F2. Typical pressure signature output.

Appendix F (Continued)

Additional Nomenclature

p_W , p_{REF} static pressure measured at wall probe, psf

p_S static pressure measured at survey probe, psf

$p_{S,O}$ static pressure measured at survey probe ahead of the model's flow field, psf

p_P static pressure measured at survey probe in model flow field, psf

p_{TS} static pressure in the test section outside the model flow field, psf

In the ideal, constant-static pressure wind-tunnel test section, each disturbance point in the model flow field pressure signature is defined by:

$$\left(\frac{\Delta p}{p}\right)_{TRUE} = \frac{p_P - p_S}{p_S} \tag{F1}$$

Obviously, this ideal cannot be met because the reference probe and the survey probe cannot occupy the same location simultaneously. So, the points in the pressure signature are obtained from:

$$\left(\frac{\Delta p}{p}\right)_{MEASURED} = \frac{p_P - p_W}{p_W} \tag{F2}$$

Equation (F1) and (F2) can be combined to obtain:

$$\left(\frac{\Delta p}{p}\right)_{TRUE} = \left(\frac{p_W}{p_S}\right)\left[\left(\frac{\Delta p}{p}\right)_{MEASURED} - \left(\frac{\Delta p}{p}\right)_{MEASURED,\,O}\right] \tag{F3}$$

where $\left(\frac{\Delta p}{p}\right)_{MEASURED,\,O}$ is the overpressure measured outside the model flow field. In an ideal wind tunnel, the total volume of the test section would be at a uniform static pressure, and

$$\left(\frac{\Delta p}{p}\right)_{TRUE} = \left(\frac{\Delta p}{p}\right)_{MEASURED}$$

because

$$p_W = p_{S,0} = p_S \qquad \text{and} \qquad \left(\frac{\Delta p}{p}\right)_{MEASURED,\,O} = 0.0$$

Whitham theory, reference 4, is used to predict $\Delta p / p$ in a uniform atmosphere from:

$$\frac{\Delta p}{p} = \frac{\gamma M^2}{\sqrt{2\beta h}} F(y) \tag{F4}$$

where F(y) is a function of the model's volume distribution, lift distribution, and free-stream Mach number. When equation (F4) is used to predict pressure signatures, the model and the survey probe(s) are assumed to be in a constant and equal static pressure field. Static pressures listed in TABLE 1 show significant static pressure differences between the flow over the survey probes, and the reference-probe in both test facilities.

Appendix F (Concluded)

TABLE 1. Facility Reference and Test Section Static Pressures.

Langley Research Center (LaRC) Unitary Plan Wind Tunnel Facility

h, inches	9.0	13.5	18.0	22.5	27.0[1]
p_{REF}, psf	169.7	169.6	169.5	169.5	169.5
p_{TS}, psf	161.2	161.1	159.7	159.7	160.0

John Glenn Research Center (JGRC) 10 ft x 10 ft Supersonic Wind Tunnel Facility

h, inches	22.5	45.0	67.5	88.9
p_{REF}, psf	152.0	152.2	152.2	152.2
p_{TS}, psf	148.2	149.3	149.5	149.3

The listed static pressures were obtained by averaging the measured static pressure values and rounding off to the nearest tenth.

The differences between p_{REF} and p_{TS} in each test section were due to the reference probe location on the side wall. Differences between p_{REF} and p_{TS} in the two wind tunnel facilities were due to the different total temperatures and total pressures at which the two wind tunnels operated. Total temperatures in the wind tunnels of the LaRC facility and the JGRC facility were 125 deg.F. and 92 deg.F. respectively, although both wind tunnels were operating at a Mach Number of 2 and a Reynolds Number of 2 x 10^6 / foot during the measurement of the pressure signatures.

The flight-track survey probe was directly under and behind the wind-tunnel model, and both model and survey probe were in the same plane along the center of the test section. Thus, it was assumed that both were in the same static pressure field, i.e. $p_{TS} = p_S$. Corrections to the nose-shock $\Delta p / p$ were made by using equation (F3) after they were adjusted for measurement "rounding". Impulse calculations were corrected in a similar manner, but the nose shocks did not need to be adjusted. With this technique, all the measured overpressures reflected the presumed uniform-pressure flow between model and the survey probe. This data could now be compared with the data obtained at any other wind-tunnel facility, once that data was similarly corrected. Similar equations would correct the overpressures measured by the other survey probes in the test section. The parameter $p_{S,O}$ at each of the survey probes would be obtained from

$$p_{S,O} = p_W\left[1.0 + \left(\frac{\Delta p}{p}\right)_{MEASURED,\,O}\right] \qquad \text{(F5)}$$

The overpressure ratio at the survey probes would be obtained from equations (F3) and (F5).

1. Used for nose shock measurements only.

REPORT DOCUMENTATION PAGE

Form Approved
OMB No. 0704-0188

1. REPORT DATE *(DD-MM-YYYY)*	2. REPORT TYPE	3. DATES COVERED *(From - To)*
01- 11 - 2006	Technical Memorandum	

4. TITLE AND SUBTITLE

Determination of Extrapolation Distance With Pressure Signatures Measured at Two to Twenty Span Lengths From Two Low-Boom Models

5a. CONTRACT NUMBER

5b. GRANT NUMBER

5c. PROGRAM ELEMENT NUMBER

6. AUTHOR(S)

Mack, Robert J.; and Kuhn, Neil S.

5d. PROJECT NUMBER

5e. TASK NUMBER

5f. WORK UNIT NUMBER

984754.02.07.07

7. PERFORMING ORGANIZATION NAME(S) AND ADDRESS(ES)

NASA Langley Research Center
Hampton, VA 23681-2199

8. PERFORMING ORGANIZATION REPORT NUMBER

L-19302

9. SPONSORING/MONITORING AGENCY NAME(S) AND ADDRESS(ES)

National Aeronautics and Space Administration
Washington, DC 20546-0001

10. SPONSOR/MONITOR'S ACRONYM(S)

NASA

11. SPONSOR/MONITOR'S REPORT NUMBER(S)

NASA/TM-2006-214524

12. DISTRIBUTION/AVAILABILITY STATEMENT

Unclassified - Unlimited
Subject Category 71
Availability: NASA CASI (301) 621-0390

13. SUPPLEMENTARY NOTES

An electronic version can be found at http://ntrs.nasa.gov

14. ABSTRACT

A study was performed to determine a limiting separation distance for the extrapolation of pressure signatures from cruise altitude to the ground. The study was performed at two wind-tunnel facilities with two research low-boom wind-tunnel models designed to generate ground pressure signatures with "flattop" shapes. Data acquired at the first wind-tunnel facility showed that pressure signatures had not achieved the desired low-boom features for extrapolation purposes at separation distances of 2 to 5 span lengths. However, data acquired at the second wind-tunnel facility at separation distances of 5 to 20 span lengths indicated the "limiting extrapolation distance" had been achieved so pressure signatures could be extrapolated with existing codes to obtain credible predictions of ground overpressures.

15. SUBJECT TERMS

Sonic boom; Whitham theory; Signature extrapolation; Wind-tunnel models

16. SECURITY CLASSIFICATION OF:			17. LIMITATION OF ABSTRACT	18. NUMBER OF PAGES	19a. NAME OF RESPONSIBLE PERSON
a. REPORT	b. ABSTRACT	c. THIS PAGE			STI Help Desk (email: help@sti.nasa.gov)
					19b. TELEPHONE NUMBER *(Include area code)*
U	U	U	UU	37	(301) 621-0390